Stratigraphy, facies analysis and sequence stratigraphy of the Eocene succession in the Shabrawet area (north Eastern Desert, Egypt): an example for a tectonically influenced inner ramp carbonate platform

E. Sallam, H. A. Wanas & R. Osman

Arabian Journal of Geosciences

ISSN 1866-7511

Arab J Geosci
DOI 10.1007/s12517-015-1969-2

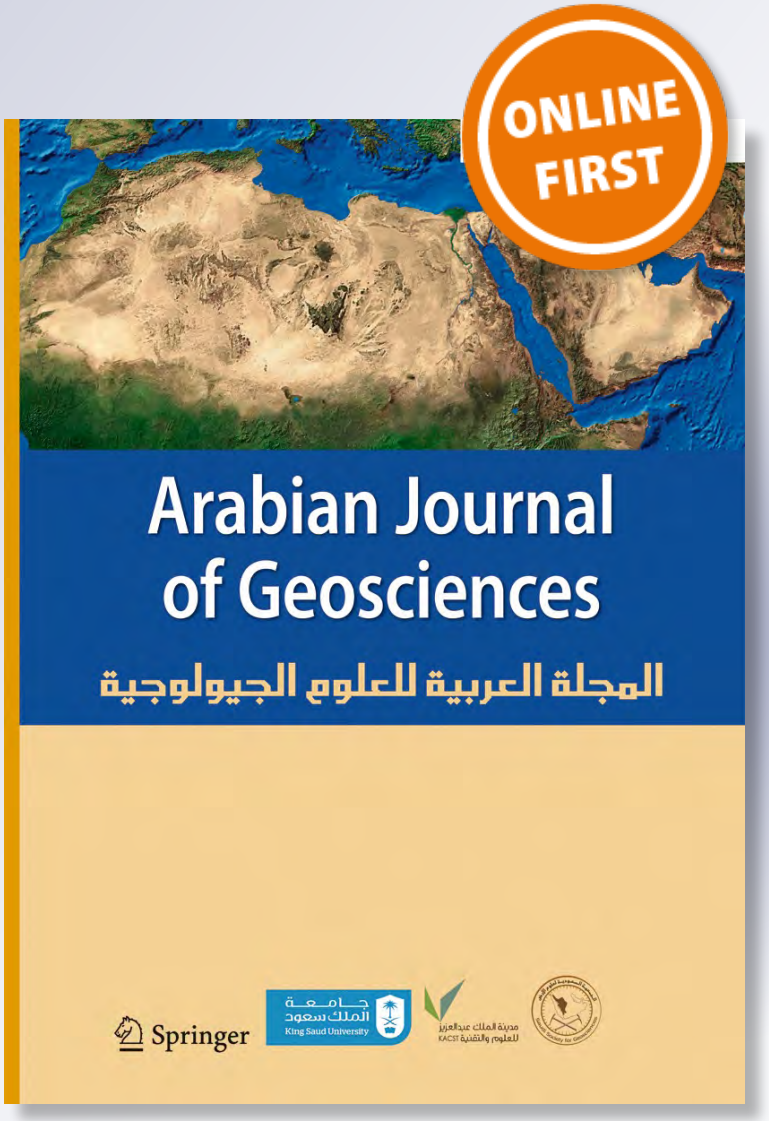

Springer

Arab J Geosci
DOI 10.1007/s12517-015-1969-2

ORIGINAL PAPER

Stratigraphy, facies analysis and sequence stratigraphy of the Eocene succession in the Shabrawet area (north Eastern Desert, Egypt): an example for a tectonically influenced inner ramp carbonate platform

E. Sallam[1] · **H. A. Wanas**[2] · **R. Osman**[1]

Received: 20 January 2015 / Accepted: 21 May 2015

Abstract The Eocene rocks in the Shabrawet area (north Eastern Desert, Egypt) have been subdivided into three formations that are from base to top: the Minia Formation (Late Ypresian), the Sannor Formation (Bartonian) and the Maadi Formation (Priabonian). These three formations are disconformable with each other. In addition, the whole Eocene succession is disconformably overlain by the Oligocene rocks and is underlain by the Cretaceous rocks with an angular unconformity surface. The Sannor Formation has been subdivided into three informal units: lower, middle and upper units. The overall sedimentary nature of the Eocene rocks in the study area is dominated by carbonate-siliciclastic rocks. Detailed microfacies analysis has enabled discrimination of 22 sedimentary microfacies types, which are grouped into six facies associations, equivalent to six depositional environments sited on an inner ramp setting. These depositional environments are floodplain-dominated fluvial, lacustrine/palustrine, tidal flat, restricted inner lagoon, shoal bar and outer lagoon with open circulation. A suitable depositional model of the Eocene rocks is given. In addition, four discrete benthonic foraminiferal biozones were reported in the Eocene succession, arranged from base to top: (1) *Alveolina frumentiformis* biozone (Late Ypresian), (2) *Orthoplecta clavata* biozone (Bartonian), (3) *Dictyoconus aegyptiensis* biozone (Bartonian) and (4) *Discorbis vesicularis* biozone (Priabonian). In terms of sequence stratigraphy, the studied Eocene succession exhibits three superimposed depositional sequences, each of which shows retrogradational (transgressive systems tract) and aggradational (highstand systems tract) to progradational (lowstand systems tract) packages of facies. The retrogradational package displays a predominance of outer lagoon and restricted inner lagoon facies. The aggradational package shows an increase of shoal bar and tidal flat facies, whereas the progradational package marks the occurrence of continental facies (floodplain-dominated fluvial and lacustrine deposits). In this study, it is noticed that there are lateral and vertical changes in the depositional environments of the Eocene rocks, between shallow marine and continental environments. Also, many unconformities have been recorded in between and within these rock units. Such remarks indicate that the Eocene rocks were deposited within a highly tectonically active area that was consequently influenced by the transgression and regression of the Neo-Tethys. Such tectonic activity could be related to the Syrian Arc System that was renewed and enlarged several times during the Late Cretaceous up to the Neogene in the eastern and southeastern Mediterranean domain.

Keywords Lithostratigraphy · Facies analysis · Depositional environments · Sequence stratigraphy · Eocene · Shabrawet area · Egypt

✉ E. Sallam
emadgeol@yahoo.com

H. A. Wanas
hamdallawanas@yahoo.com

[1] Department of Geology, Faculty of Science, Benha University, Benha, Egypt

[2] Department of Geology, Faculty of Science, Menoufiya University, Shebin El-Kom, Egypt

Introduction

The Shabrawet area lies close to the Suez Canal, between Ismailia and Suez (about 40 km south of Ismailia and about

Published online: 03 June 2015

137 km to the northeast of Cairo). The area is bounded from the east by the plain of the Great Bitter Lake. It is located between latitudes 31° 09¯ and 31° 20¯ N and longitudes 32° 12¯ and 32° 27¯ E (Fig. 1a). The exposed rocks in the Shabrawet area range in age from the Early Cretaceous to the Recent (Fig. 1b).

The Shabrawet area was a target of many geological studies dealt usually with its structural setting. Among these studies is the pioneer work of Al-Ahwani (1982) who introduced a detailed study of the structural analysis and tectonic evolution of this area. However, few studies dealt with the stratigraphy and depositional modeling of the Eocene rocks in the Shabrawet area (Al-Ahwani 1982; Mohammad and Omran 1991; Shamah and Helal 1993a, b; Abu El-Ghar 2007; Selim et al. 2012). In this context, the literature review reflects a paradox ages of the Eocene rock units. There are some authors (e.g. Osman 2003; Abu El-Ghar 2007; Issawi et al. 2009) who believed in the presence of Lower, Middle and Upper Eocene rocks in the north Eastern Desert in general and in the Shabrawet area in particular, whereas others (e.g. Sadek 1926; El-Akkad and Abdallah 1971; Al-Ahwani 1982; Shamah and Helal 1993a, b; Haggag 2010) believed that only Middle Eocene rocks are exposed in the Cairo–Suez district including the study area. Table 1 shows a comparison between the Eocene stratigraphic subdivisions used by different authors in the Shabrawet area and some other localities in the North Eastern Desert of Egypt.

The present work aims to study the stratigraphy of the Eocene rocks exposed in the Shabrawet area and to infer their depositional environments and sequence stratigraphic elements. Constructing a suitable depositional model for the Eocene rocks is one of the targets of the present work. To achieve these targets, detailed field observations and petrographic investigations of the studied Eocene rocks have been done. In addition, the larger benthic foraminifera (LBFs) were identified to assign the relative ages and biostratigraphic zonation of the Eocene rock units.

Methods of study

Five lithostratigraphic sections of the Eocene rocks in the study area were measured, sampled and described (Fig. 1). These sections are located at: (1) El-Goza El-Hamra (EGH) (30° 16¯ 57.34¯ N, 32° 18¯ 30.97¯ E); (2) Geneifa (GEN) (30° 12¯ 27.77¯ N, 32° 22¯ 48.54¯ E); (3) Fanara (FAN) (30° 16¯ 04.65¯ N, 32° 19¯ 18.46¯ E); (4) Darbet El-Houity (DEH) (30° 16¯ 10.12¯ N, 32° 17¯ 40.10¯ E) and (5) South Shabrawet West (SSW) (30° 15¯ 57.77¯ N, 32° 14¯ 58.54¯ E). The petrographic examination was carried out on 120 thin sections;

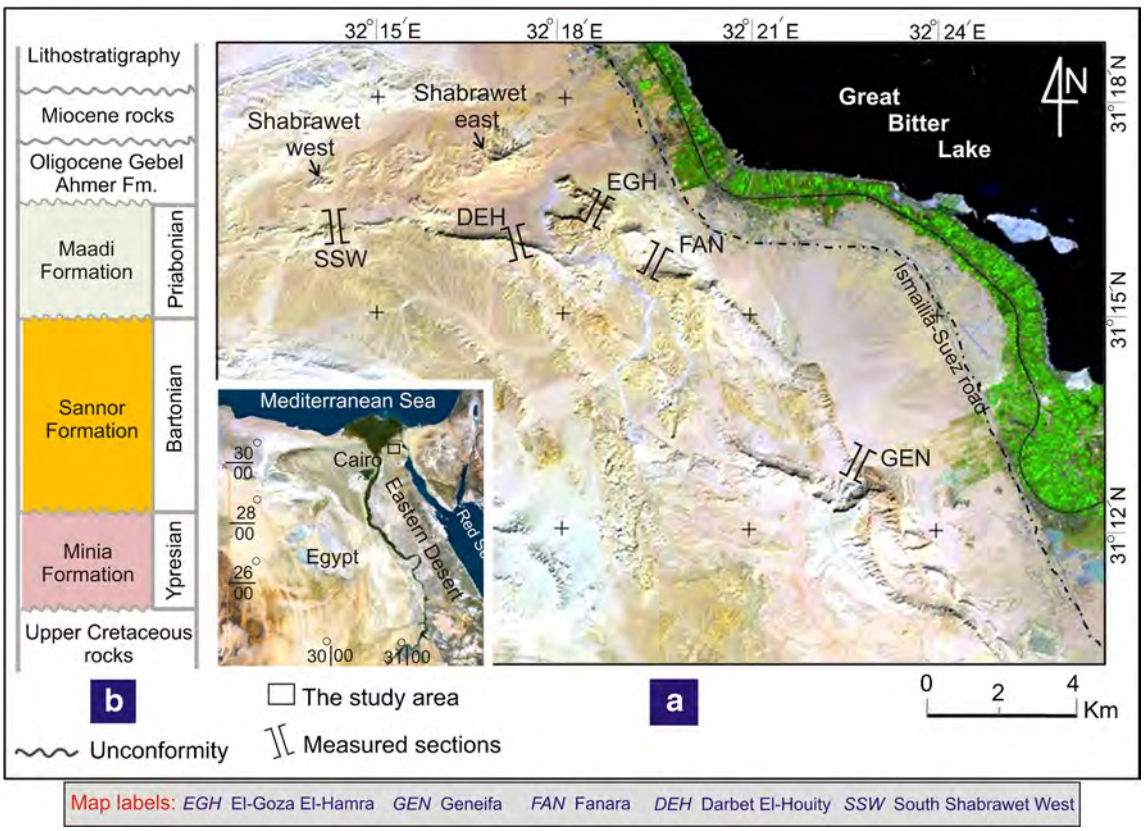

Fig. 1 **a** ETM^{+} image of the Shabrawet area showing the location of the studied sections. **b** Lithostratigraphic column of the exposed Eocene rock units in the Shabrawet area. *EGH* El-Goza El-Hamra, *GEN* Geneifa, *FAN* Fanara, *DEH* Darbet El-Houity, *SSW* South Shabrawet West

Table 1 Correlation chart showing the Eocene rock units in the Shabrawet area and its adjacent localities in the North Eastern Desert, Egypt

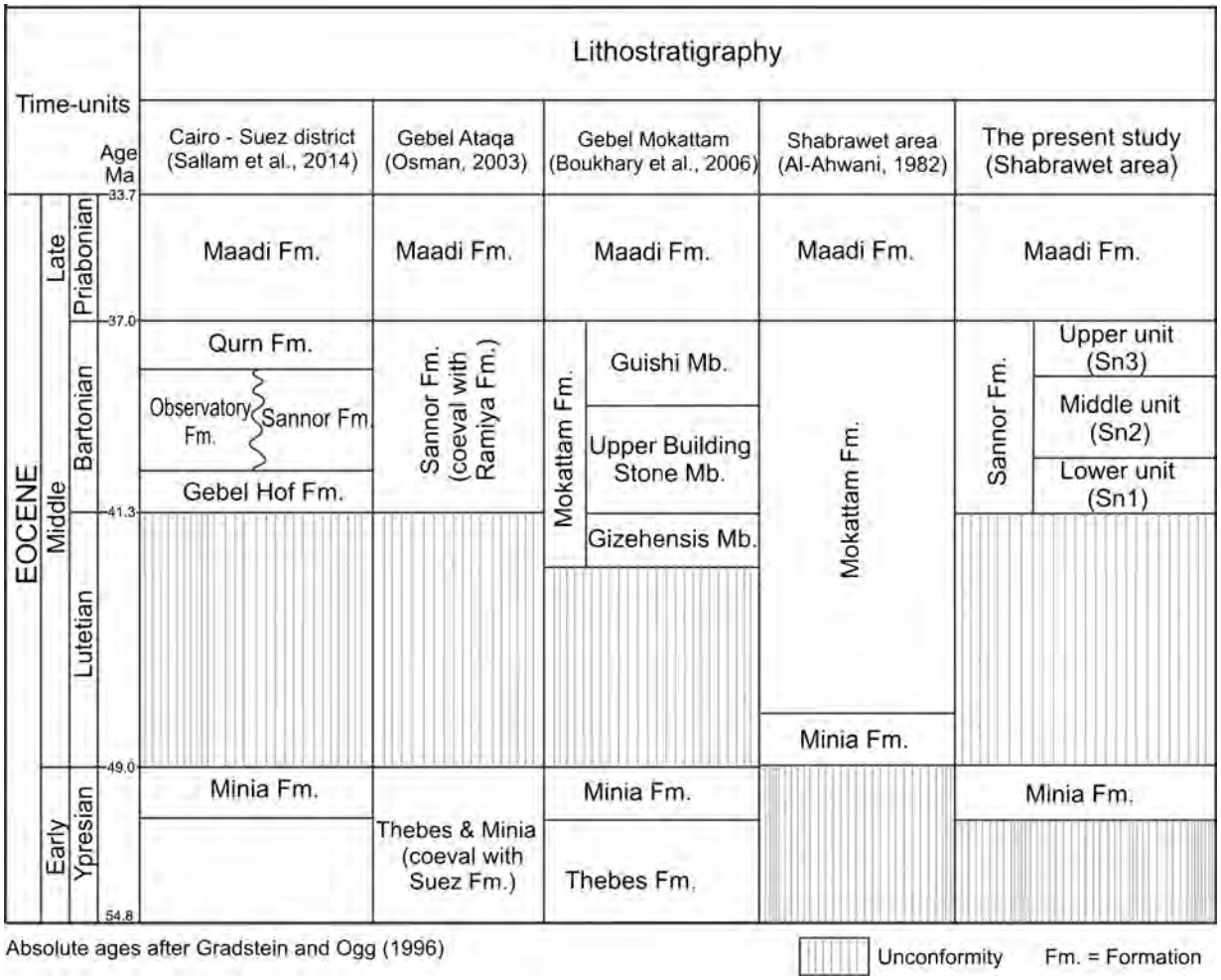

another set (18 slides) of uncovered thin sections was stained with Alizarin Red S to differentiate between dolomite and calcite. The petrographic study is used to infer the microfacies types and identify the larger benthic foraminifera in the studied rocks. The sandstone types and limestone microfacies were described following the classification of Pettijhon et al. (1973) and Dunham (1962), respectively.

Geologic setting

The Shabrawet area is located in the north Eastern Desert of Egypt (Fig. 1). It is greatly influenced by the Syrian Arc movement, the End Lutetian Pyrenean–Atlasic event and the rifting of the Gulf of Suez (Moustafa and Khalil 1989). The "Syrian Arc System" was recognized by Krenkel (1925–1934) in the eastern and southeastern Mediterranean domains. This system was renewed and enlarged several times during the Late Cretaceous up to the Neogene. The development of the Shabrawet fold belt in the study area is related to these orogenic movements (Al-Ahwani 1982; Haggag 2010 and others).

According to Al-Ahwani (1982), the structural pattern of the Shabrawet area comprises two asymmetrical anticlines, namely, Shabrawet east and Shabrawet west, enclosing a shallow syncline in between. The axes of these anticlines are running in the NE–SW direction. The Shabrawet east anticline plunges to the SW, whereas the Shabrawet west anticline is double plunged to the NE and SW directions. The core of the Shabrawet east anticline is covered by Lower Cretaceous ferruginous sandstone, whereas the core of the Shabrawet west anticline is covered by Cenomanian marine rocks. The southern limbs of the two anticlines are covered by a thick sequence of the Eocene rocks, but the northern limbs are covered by the Miocene rocks. The synclinal basin in between the two Shabrawet anticlines is filled by Upper Cretaceous–Lower Tertiary continental strata that showed pedogenic modifications (Wanas and Abu El-Hassan 2006). The Shabrawet area is highly faulted being affected by two major fault trends,

which were delineated by Al-Ahwani (1982) as follows: the older NE–SW faults greatly affected the Cretaceous strata in both Shabrawet anticlines, prior to the deposition of the Eocene rocks, whereas the younger NW–SE faults (clysmic) led to many Eocene scarps present in the study area.

Lithostratigraphy

The Shabrawet area has a thick sedimentary succession ranging in age from the Early Cretaceous to the Recent (Al-Ahwani 1982; Mohammad and Omran 1991; Haggag 2010 and others). The Cretaceous rocks build the main bulk of both Shabrawet anticlines, whereas the relatively younger rocks (Eocene, Oligocene and Miocene) constitute several dissected scarps around these anticlines (Fig. 2).

The studied Eocene rocks crop out south, southwest and southeast of the two Shabrawet anticlines. These rocks constitute a relatively high scarp (elevation 300–500 m a.s.l.) extending between Gebel El-Goza El-Hamra (located few kilometers southwest of Fayed City) and Gebel Geneifa (opposite Geneifa town) (Fig. 1a). In the study area, the Eocene succession is punctuated by several unconformities. Many of these unconformities are mainly structurally controlled, and few of them are more related to the eustatic movements of the sea level (Al-Ahwani 1982; Haggag 2010). The Eocene rocks in the Shabrawet area are divided into three formations. These are from base to top (Fig. 3): the Minia Formation (Late Ypresian), the Sannor Formation (Bartonian) and the Maadi

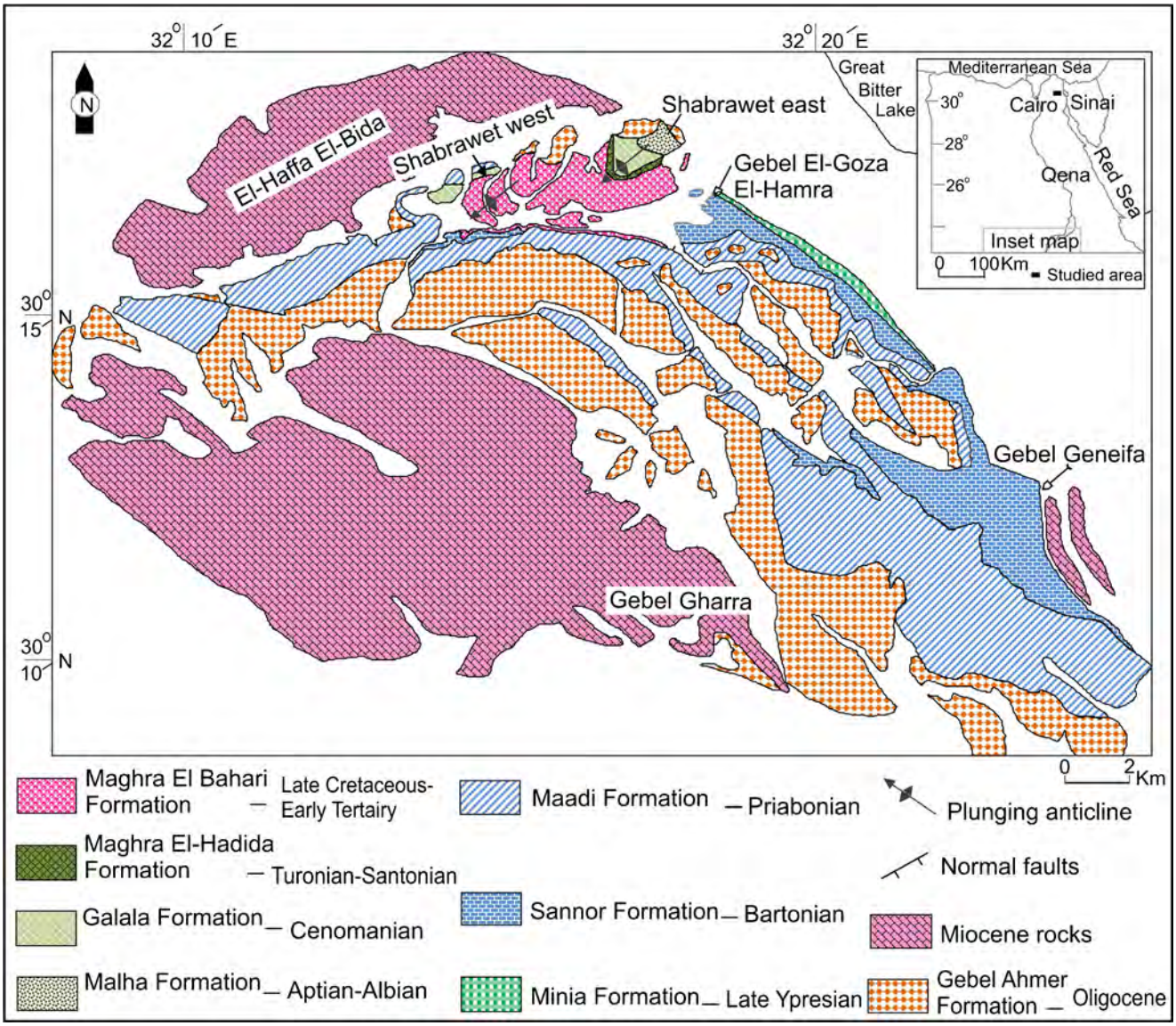

Fig. 2 Geological map of the Shabrawet area and its surroundings (modified after Al-Ahwani 1982; Haggag 2010)

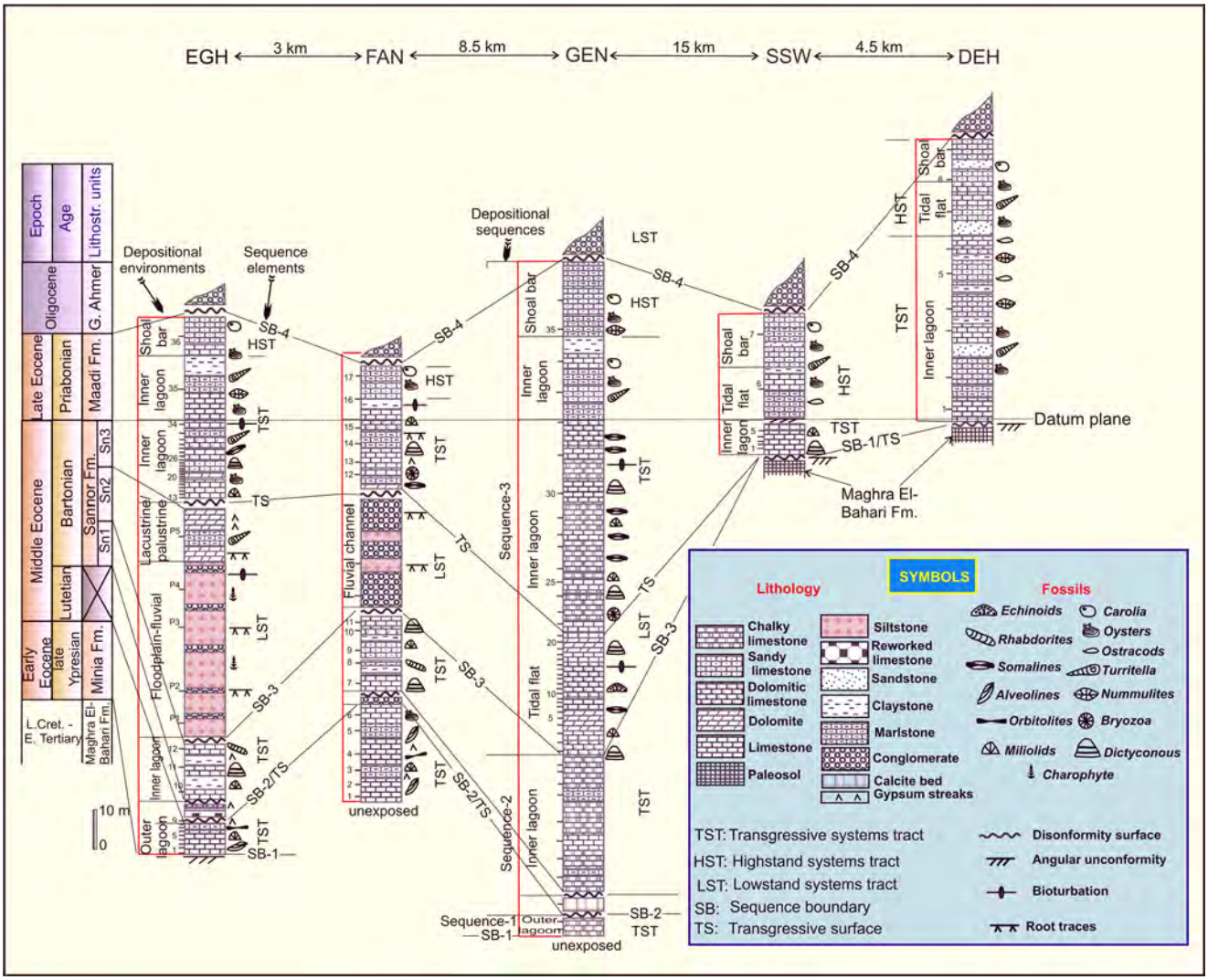

Fig. 3 Stratigraphic correlation chart showing the lithologic characteristics and sequence stratigraphic elements of the Eocene rocks in the study area

Formation (Priabonian). The following is a detailed description of these formations.

The Minia Formation (Late Ypresian: Cuisien)

The Minia Formation was first introduced by Said (1960) to describe the alveolinal limestone section (35 m thick) at Zawiet Saada, opposite Minia City, and the Middle Eocene (Early Lutetian) age was given to it. Based on larger benthic foraminifera, Boukhary and Abdelmalik (1983) attributed this formation to the Late Early Eocene (Late Ypresian). The Minia Formation shows angular unconformity with its underlying Cretaceous strata (Al-Ahwani 1982; Abu El-Ghar 2007). In the present study, the thickness of the Minia Formation is 26, 9.0 and 5.0 m at Fanara, El-Goza El-Hamra and Geneifa sections, respectively (Fig. 4a). At the other two studied sections (Darbet El-Houity and South Shabrawet West), the Minia Formation is absent. The sub-horizontal beds of the Minia Formation unconformably overlie the inclined Upper Cretaceous rocks with a well-marked angular unconformity in between (Al-Ahwani 1982). However, in the studied sections, this contact is largely eroded along a NW–SE fault running along a wadi (Darbet El-Houity) draining the western scarps into the Great Bitter Lake to the east. Therefore, the basal contact of the Minia Formation is not exposed. The Upper Ypresian Minia Formation is disconformably overlain by the Bartonian Sannor Formation. At the El-Goza El-Hamra and Fanara sections, the disconformity surface is evidenced by the occurrence of a sugary crystalline gypsum layer (45 cm thick) at the base, followed upward by 4.0 m thick of reworked limestones and white gypsum, and covered by a yellowish grey and reddish, ferricrete horizon (0.20 m thick). The ferricrete horizon is topped by a 0.5-m-thick basal conglomerate mainly of reworked limestone and dolomite pebbles, embedded in a clayey sand matrix. At the base of the Geneifa section, the Upper Ypresian Minia Formation is separated

from its overlying Bartonian Sannor Formation by a thick, dark grey, smoky, blocky calcite bed (2.0 m thick) (Fig. 4b). Lithologically, the Minia Formation in both the El-Goza El-Hamra and Fanara sections consists mainly of thick-bedded, pinkish to yellowish and whitish grey, algal/alveolinal limestones at the base, grading upward into thin-bedded, yellowish grey, marly limestones intercalated with gypseous shales. The alveoline tests are large elongated shape, medium to coarse grained and variable in length (from 0.5 to 2.0 cm). The alveoline tests are well organized and oriented parallel to the bedding planes. At the Geneifa section, the Minia Formation is composed mainly of white, thin-bedded, chalky limestones that are highly dissected by gypsum streaks and largely disseminated by well crystalline, nodular gypsum pockets. The gypsum streaks, each of which is 7.0 cm thick, sometimes occur as parallel layers or as a network intersecting each other. A relatively thin limestone bed (50 cm thick) full of badly preserved oyster shells is recorded in the middle part of the Minia Formation at the Geneifa section.

The rocks of the Minia Formation are rich in larger benthic foraminifera and Miliolidae, e.g. *Alveolina frumentiformis* Schwager, *Assilina praespira* Douville, *Orbitolites* cf. *complanatus* Lamarck, *Discocyclina* sp., *Pyrgo bulloides* Brady, *Quinqueloculina seminula* Linne, *Lenticulina* (*Rubulus*) sp., *Ruessella terquemi* Cushman and *Ruessella elongata* Terquem. Some calcareous red algae (e.g. *Rhodophyta*) occur also. These fossils are of Late Ypresian in age (Boukhary and Abdelmalik 1983).

The Minia Formation could be equivalent to the Suez Formation (El-Akkad and Abdallah 1971) at Gebel Ataqa on the northwest side of the Gulf of Suez. The age of the Suez Formation is Middle Eocene (Lutetian) according to El-Akkad and Abdallah (op. cit), but Osman (2003) assigned the Early Eocene (Late Ypresian) age to this formation for the presence of *O.* cf. *complanatus* Lamarck. The confusion originated when the age of the Suez Formation was wrongly decided to the Middle Eocene for the mis-identification of the *Orbitolites*, which was considered coeval with *Nummulites gizehensis* of Middle Eocene age (Sadek 1926).

The Sannor Formation (Bartonian)

The Sannor Formation was introduced by Boukhary and Abdelmalik (1983) for its type section in the Nile Valley at the latitude of Beni Suef, and it was assigned the Bartonian age. In the study area, the Sannor Formation assumes distinct lithology and fossil content distinguishing it from the older and younger rocks. At the El-Goza El-Hamra section, the Sannor Formation occurs as isolated conical hills with steep slopes and rounded to nearly flat-topped crests (Fig. 5a). The maximum thickness (about 130 m thick) of the Sannor Formation occurs at the Geneifa section. Northward, in the El-Goza El-Hamra and Fanara sections, the thickness of the Sannor Formation decreases to about 100 and 64 m, respectively. At the Darbet El-Houity section, the Upper Cretaceous–Lower Tertiary Maghra El-Bahari Formation is disconformably overlain by the Upper Eocene Maadi Formation.

On the basis of its lithological characteristics, the Sannor Formation is subdivided into three informal units (Fig. 5b): lower, middle and upper units. At the Geneifa section, the lower unit of the Sannor Formation (Sn_1) consists mainly of about 45 m thick of thin-bedded, white chalky limestone with few hard dolomitic limestone interbeds (Fig. 5c). In both the EGH and FAN sections, the Sn_1 is composed of about 20 m thick of brownish green claystones interbedded with foraminiferal limestones (rich in *Dictyoconus aegyptiensis* and *Idalina cuvillieri*) and highly dissected by gypsum streaks.

The middle unit of the Sannor Formation (Sn_2) displays lateral lithofacies changes, from siliciclatic rocks in both the El-Goza El-Hamra and Fanara sections in the north to dolomitic limestone at the Geneifa section to the south. It is laterally pinched out due south and southwest directions and disappears totally at the Geneifa, Darbet El-Houity and South

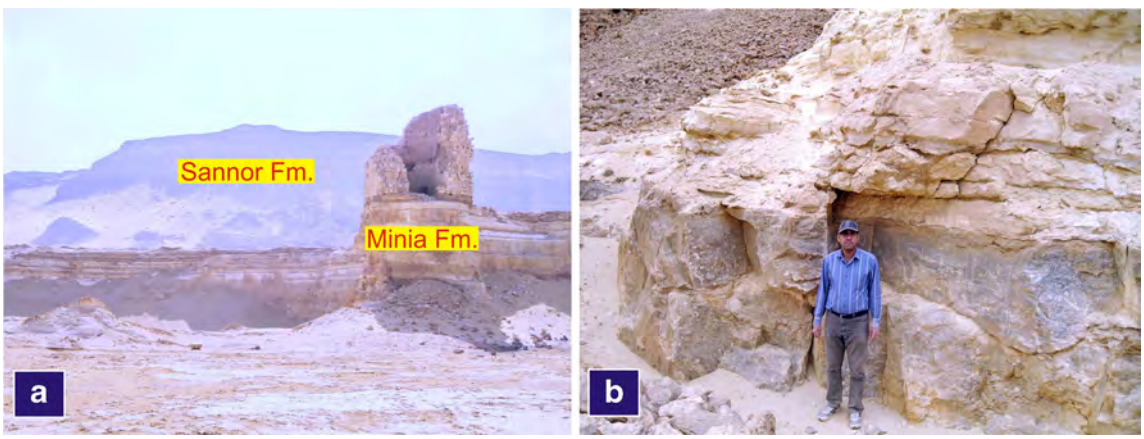

Fig. 4 Field photographs showing **a** thick-bedded alveolinal limestones of the Minia Formation overlain by the Sannor Formation, EGH section, and **b** a thick-bedded, smoky, dark grey calcite bed between the Minia Formation (*below*) and the Sannor Formation (*above*), GEN section

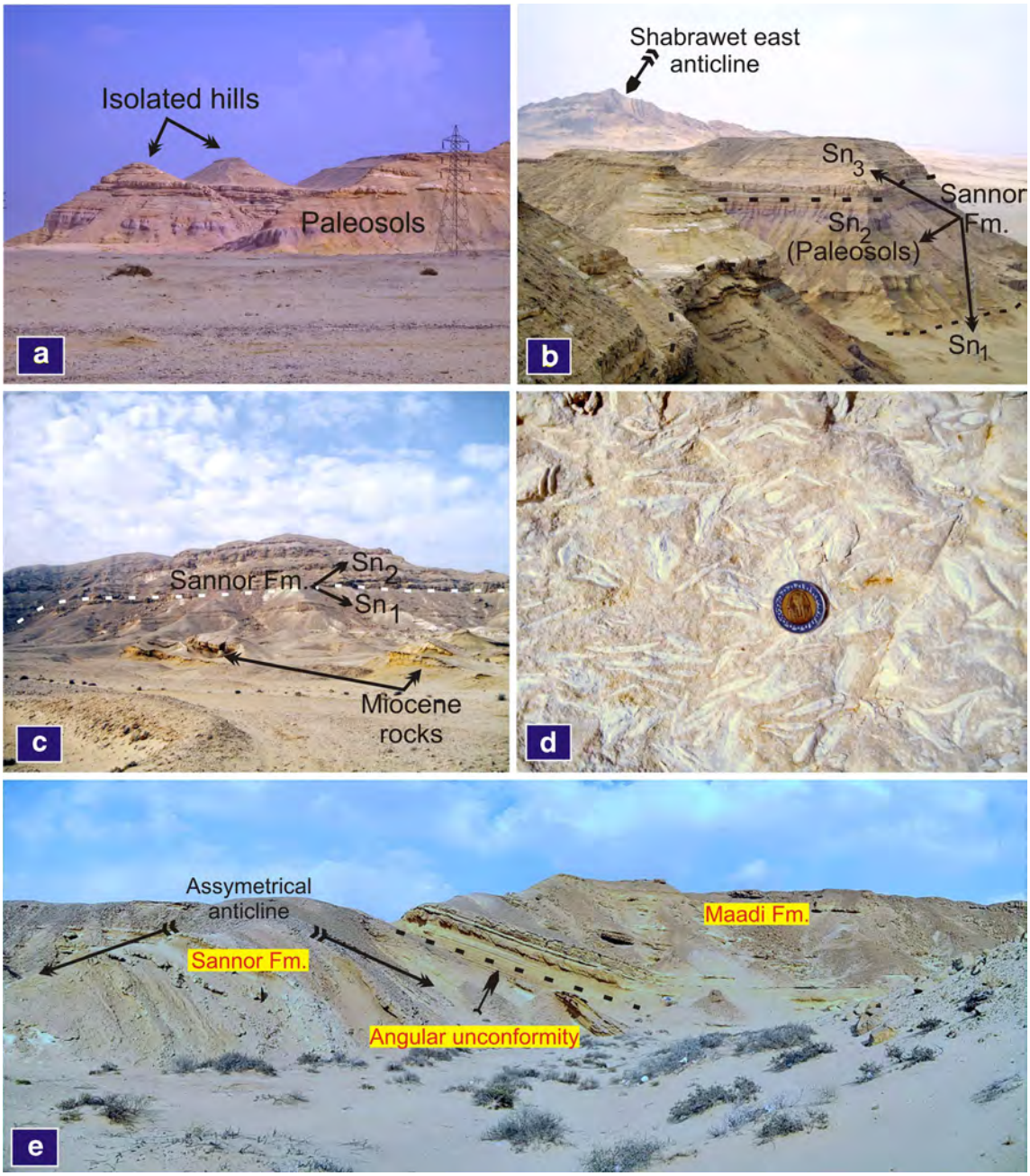

Fig. 5 Field photographs showing **a** isolated conical hills of the Sannor Formation, Gebel El-Goza El-Hamra; **b** units of the Sannor Formation abutting against the deformed Cretaceous rocks of the Shabrawet east anticline, EGH section; **c** the Bartonian Sannor Formation abuts against the younger Miocene rocks, GEN section; **d** *Somalina*-carrying limestone in the upper unit (Sn_3) of the Sannor Formation, GEN section; and **e** angular unconformity between folded beds of the Sannor Formation and the sub-horizontal beds of its overlying Maadi Formation, SSW section

Shabrawet West sections (Fig. 3). At the El-Goza El-Hamra section, the Sn_2 occurs as a siliciclastic wedge-like unit within the Bartonian limestones assuming a thickness of about 60 m. At this locality, the Sn_2 is composed mainly of about 45 m thick of claystone, siltstone and coarse-grained sandstone that are interbedded with conglomerate and topped by about 15 m thick of thin-bedded dolomite and marlstone, including root casts. These rocks are barren of fossils except some small gastropod fossils in the upper marlstone beds. They exhibit pedogenic features such as colour mottling, root traces and desiccation cracks. However, these deposits are not dealt with in great detail in this work and they could need further detailed sedimentological studies. At the Fanara section, the Sn_2 consists mainly of 24 m thick of sandy conglomerates interbedded

with sandstones and claystones. The conglomerates consist of sub-rounded to sub-angular, brownish grey dolomitic limestone and quartz pebbles, embedded in a matrix of coarse-grained sand. The sandstone is ferruginous and includes root traces. On the other hand, at the Geneifa section, the Sn_2 is made up of about 30 m thick of dolomite alternated with dolomitic limestone, including few marlstone and shale intercalations. The limestone is fossiliferous, hard and grey to whitish grey in colour.

The upper unit of the Sannor Formation (Sn_3) assumes more or less steep cliffs. At the Geneifa section, it consists mainly of about 20 m thick of bryozoan/foraminiferal limestone, followed upward by about 35 m thick of white chalky limestone carrying *Somalina stefaninii* Silvestri (Fig. 5d). At the El-Goza El-Hamra and Fanara sections, the Sn_3 is composed mainly of about 20 m thick of thin-bedded, whitish grey, bioturbated, fossiliferous limestone with several dolomite interbeds. The dolomite is vuggy, dull to dark grey, hard and ledge forming. The Sn_3 disconformably overlies the siliciclastic beds of the Sn_2 and is disconformably overlain by the Maadi Formation. At the South Shabrawet West section, the Sn_3 consists of about 8.0 m thick of grey to yellowish grey, hard, foraminiferal limestone intercalated with thin sandy limestone interbeds. At this locality, the Sn_3 disconformably overlies the Upper Cretaceous–Lower Tertiary Maghra El-Bahari Formation and is overlain by the Upper Eocene Maadi Formation with an angular unconformity in between (Fig. 5e).

In the present work, the stratigraphic position of the Sn_2 between the two Bartonian units (Sn_1 and Sn_3) proves the development of the Sn_2 within the Bartonian age. This is closely similar to that recorded by Sallam et al. (2015) during their study for the Eocene succession in the Cairo–Suez district, Egypt.

Palaeontologically, the Sannor Formation has a high-diversified community of larger benthic foraminifera, such as *S. stefaninii* Silvestri, *D. aegyptiensis* (Chapman), *I. cuvillieri* Bignot and Strougo, *Rhabdorites minima* (Henson), *O.* cf. *complanatus* Lamarck, *Planotrillina deserti* Bignot and Strougo, *Planorbulina* sp., *Gypsina carteri* and *Linderina* cf. *brugesi*. It also includes several species belonging to the Miliolidae, e.g. *Pseudolacazina schwagerinoides* (Blanckenhorn), *P. deserti* Bignot and Strougo, *Pyrgo* cf. *bulloides* (d'Orbigny), *Valvulina* gr. *schwageri* Chapman, *Peneroplis dusenbury* Henson, *Periloculina* cf. *dalmatina* Drobne, *Quiqueloculina* sp., *Triloculina* sp. and *Biloculina* sp. Two bank beds laden with *Vulsella* sp., *Natica longa*, *Gisortia gigantea* and *Turritella* sp. occur at the topmost part of the Sn_3 of the Sannor Formation in the El-Goza El-Hamra and Fanara sections. These fossil assemblages suggest Bartonian age of the Sannor Formation. Therefore, it could be equivalent with the Observatory Formation in Helwan area (Farag and Ismail 1959), the Guishi Formation at Gebel Mokkatam (Said and Martin 1964) and the Ramiya Formation at Gebel Ataqa (El-Akkad and Abdallah 1971).

The Maadi Formation (Priabonian)

Said (1962) assigned the Late Eocene age to the Maadi Formation and correlated it with the Wadi Hof Formation described by Farag and Ismail (1959) in the Helwan area, the Qasr El-Sagha Formation (Beadnell 1905) in the Faiyum, and the Hamra Formation in the Bahariya Oasis (Said and Issawi 1964). The Maadi Formation is strikingly developed in more or less vertical steep scarps in the western and south-western parts of the study area, extending in E–W and NW–SE directions. It is characterized by a yellow to yellowish brown colour, which contrast with the underlying earthy grey, foraminiferal limestones of the Sannor Formation. The lower contact of the Maadi Formation with its underlying older beds is conformable in some sections and unconformable in others. For example, at the El-Goza El-Hamra, Fanara and Geneifa sections, the Maadi Formation overlies the Bartonian Sannor Formation with seeming conformity, whereas at the Darbet El-Houity section, the Maadi Formation disconformably overlies the Upper Cretaceous–Lower Tertiary Maghra El-Bahari Formation indicating wide stratigraphic hiatuses in this section. Otherwise, at the South Shabrawet West section, the nearly horizontal beds of the Maadi Formation (27 m thick) overlie steeply inclined and locally folded strata of the Sannor Formation, with an obvious angular unconformity (Fig. 6a). This observation of conformable and unconformable relationships between the Maadi and its underlying rock units is probably due to the continuous deposition of the Maadi Formation above the Sannor Formation in places (e.g. the El-Goza El-amra, Fanara and Geneifa sections) and the discontinuous deposition in others (e.g. the Darbet El-Houity and South Shabrawet West sections). The Maadi Formation is disconformably overlain by Oligocene continental siliciclastic succession (the Gebel Ahmer Formation) consisting mainly of coarse- to medium-grained sand, ferruginous grits and gravels rich in fossil wood (Fig. 6b). The Oligocene Gebel Ahmer Formation is easily recognized from a distance owing to its burnt dark brown, blackish gravels and varicoloured sands, which contrast with the earthy grey and yellowish brown colours of the surrounding Middle and Upper Eocene rocks.

Lithologically, the Maadi Formation is made up of a succession of siliciclastic-carbonate rocks comprising several mollusc-laden bank facies and thin bands of phosphatic sandstone with fish teeth. It attains a maximum thickness of about 70 m at Darbet El-Houity and decreases eastward and southeastward to about 20 and 15 m at the El-Goza El-Hamra and Fanara sections, respectively. Southwards, the thickness of the Maadi Formation increases again, where it reaches about 35 m thick at the Geneifa section. The Maadi Formation in the studied sections can be subdivided into three different parts on the

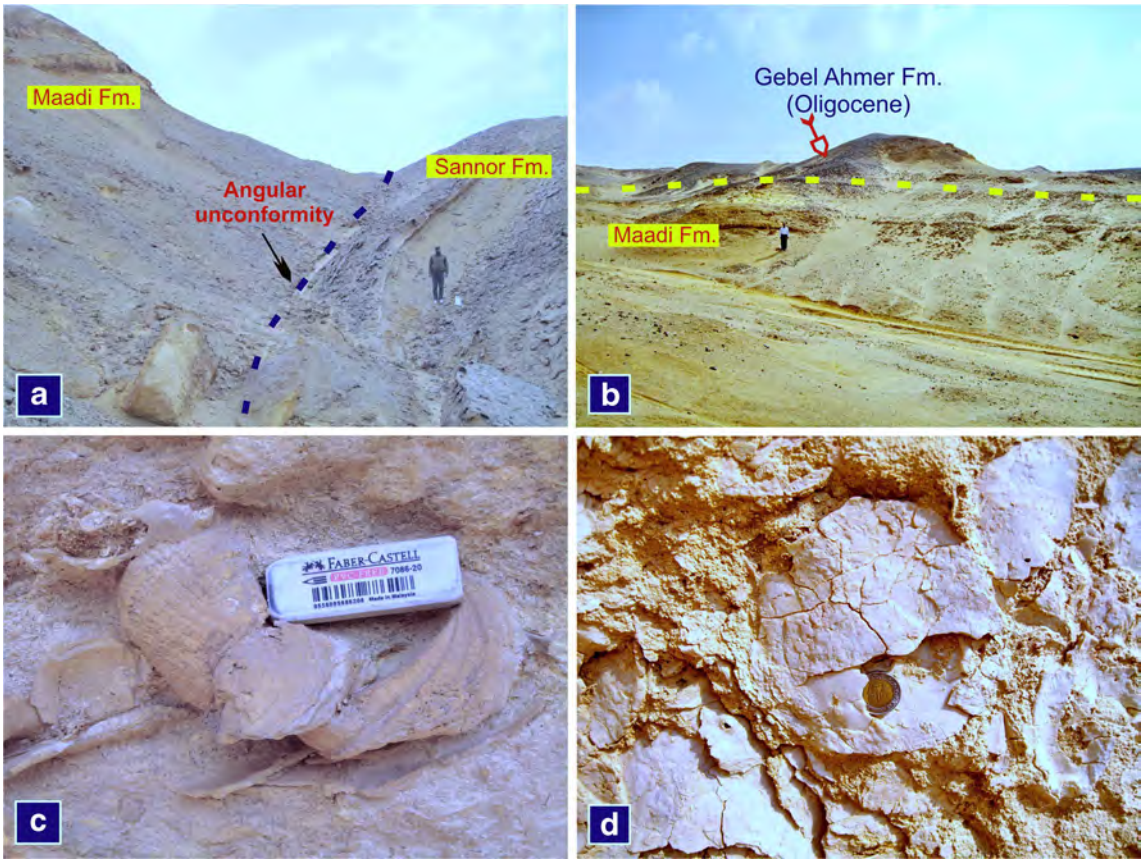

Fig. 6 Field photographs showing **a** angular unconformity between the Sannor Formation and its overlying Maadi Formation, SWW section; **b** disconformity surface between the Maadi Formation and its overlying Oligocene Gebel Ahmer Formation, EGH section; **c** *Ostrea multicostata–Gisortia* zone in the lowermost part of the Maadi Formation, EGH section; and **d** *Carolia placunoides* zone in the topmost part of the Maadi Formation, EGH section

basis of lithology and fossil content. The basal part consists mainly of thick-bedded, faint yellow and grey limestones that are rich in thick large-sized oyster shells such as *Ostrea multicostata* Deshayes, *Gisortia* spp., *Ostrea clotbeyi* Bellardi, *Vulsella crispata* Fisher, *Spondylus aegyptiacus* Newton and many others (vide infra). The middle part assumes a relatively gentle slope and consists mainly of greyish yellow, fossiliferous limestones and brownish yellow marly limestones intercalated with sandy claystone and grey sandstone interbeds, which are characterized by the abundance of *Carolia placunoides* Cantraine and subordinate *S. aegyptiacus* Newton. The limestones of the middle part yield also several species of ostracoda and benthic foraminifera. The upper part consists mainly of thick-bedded, grey limestone and greyish brown dolomitic limestone with some marl, sandstone and claystone interbeds including several oyster banks at the top. Each oyster bank assumes more or less 3.0 m thick.

The limestone beds of the Maadi Formation are rich with macro-fossils, e.g. *O. multicostata* Deshayes, *Gisortia* spp., *O. clotbeyi* Bellardi, *Ostrea fraasi*, *Ostrea roncana*, *C. placunoides* Cantraine, *V. crispata* Fisher, *S. aegyptiacus* Newton, *Turritella heluanensis*, *Turritella zitteli*, *Turritella* spp. and many others. Bryozoan remains and echinoids are also common. It was then possible to recognize four locally biostratigraphic zones in the Maadi Formation, from the base to the top: *O. multicostata–Gisortia* zone (Fig. 6c), *Turritella* zone, *Ostrea clotbei* zone and *C. placunoides* zone (Fig. 6d). Several species of Ostracoda, commonly *Asymmetricythere hiltermanni* and *Uromuellerina saidi*, were also identified associated with the four identified macro-fossil zones indicated above. These fossils suggest Late Eocene (Priabonian) age for the Maadi Formation.

Larger benthic foraminiferal biostratigraphy

Biostratigraphical studies on the carbonate platform succession at the Shabrawet area documented abundant and rich diversity of shallow marine larger benthic foraminifera during the Eocene (Shamah and Helal 1993a). They allow assigning Late Ypresian age to the Minia Formation, Bartonian to the Sannor Formation and Priabonian to the Maadi Formation.

The biostratigraphic distribution of the larger benthic foraminifera in the studied sections was correlated using the local biostratigraphic zonation given by Shamah and Helal (1993a) for the Eocene rocks in the Shabrawet area. In the present study, four discrete larger benthic foraminiferal biozones were recognized in the Eocene succession. The *A. frumentiformis* Schwager (Fig. 7a, b) biozone is restricted to the exposed part of the Minia Formation of 26, 9.0 and 5.0 m thick at the base of the Fanara, El-Goza El-Hamra and Geneifa sections, respectively, and is considered to be Late Ypresian age. Other Late Early Eocene index fossils identified together with *A. frumentiformis* are *Alveolina boscii*, *O.* cf. *complanatus* Lamarck, *A. praespira* Douville, *Discocyclina* sp., *P. bulloides* Brady, *Q. seminula* Linne, *Lenticulina* (*Rubulus*) sp., *R. terquemi* Cushman and *R. elongata* Terquem. The *Orthoplecta clavata* biozone was defined by the total range of *O. clavata* (Shamah and Helal 1993a). In the studied sections, this biozone is correlated with the lowermost part (20 m thick) of the Bartonian Sannor Formation at both the El-Goza El-Hamra and Fanara sections. The *O. clavata* biozone is highly fossiliferous with other benthic foraminifera, e.g. *Quinqueloculina juleana* d'Orbigny, *Turrilina andreai* Cushman, *Buliminelaa limbosa* Cushman & McCulloch, *Bolivina submarina* Cushman, *Epistomaria*

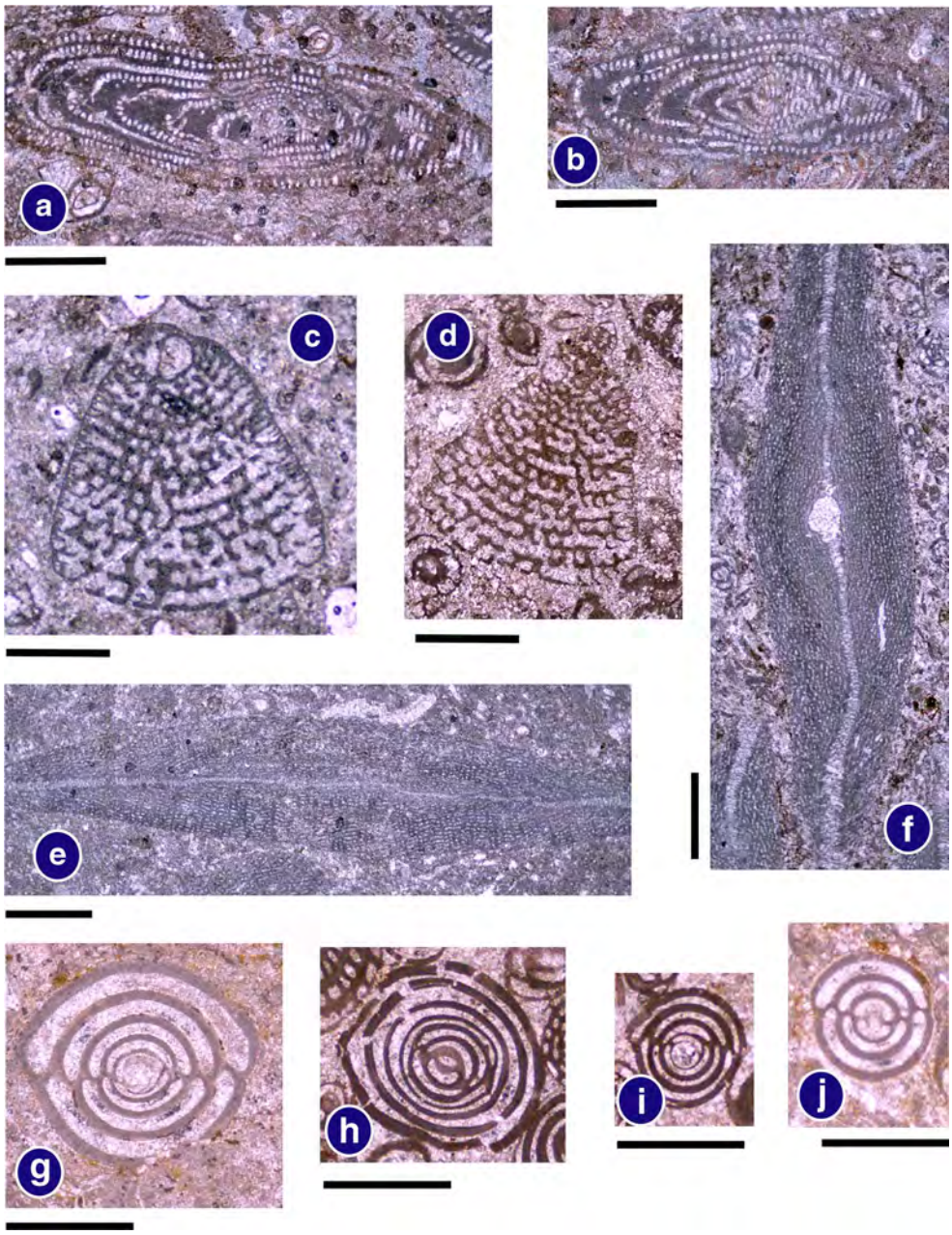

Fig. 7 Photomicrographs showing **a**, **b** *Alveolina frumentiformis* Schwager, axial sections, Minia Fm., EGH, FAN sections, samples EGH1-4, FAN1-6; **c**, **d** *Dictyoconus aegyptiensis* (Chapman), Sannor Formation, EGH, FAN, GEN, SSW sections, samples EGH10,11,25,27, FAN7,8,13, GEN22,23,24, SSW 1,2,3; **e**, **f** *Somalina stefaninii* Silvestri, Sannor Formation, EGH, GEN, FAN sections, samples EGH12,13,15, GEN20-34, FAN12,13,15; and **g**–**j** *Idalina cuvillieri* Bignot and Strougo, Sannor Formation, EGH, FAN, GEN, SSW sections, samples EGH33,34, FAN9,15, GEN8,11,14, SSW1,3,4. *Scale bar*=1 mm

rimosa Parker & Jones, *Cibicides lobatulus* Walker & Jacob, *Articulina laevigata* Terquem and *Triloculina angularis* d'Orbigny. The base of the *D. aegyptiensis* biozone is easily recognized with the first occurrences of *D. aegyptiensis* (Chapman) (Fig. 7c, d), together with the agglutinated forms *S. stefaninii* Silvestri (Fig. 7e, f), *I. cuvillieri* Bignot and Strougo (Fig. 7g–j) and *P. schwagerinoides* (Blanckenhorn) (Fig. 8a–e); all these taxa represent index fossils of the Bartonian and are restricted to the *D. aegyptiensis* biozone. In the present sections, the *D. aegyptiensis* biozone attains a thickness of about 130 m in the Sannor Formation. This zone is associated with other larger benthic foraminifera and miliolids, e.g. *R. minima* (Henson) (Fig. 8f), *P. dusenbury* Henson (Fig. 8g), *P.* cf. *bulloides* (d'Orbigny), *V.* gr. *schwageri* Chapman (Fig. 8h), *P. deserti* Bignot and Strougo (Fig. 8i–k), *P.* cf. *dalmatina* Drobne, *G. carteri*, *L.* cf. *brugesi*, *Quiquelocolina seminula* Linne and *Rotalia audiuini* d'Orbigny. The foraminiferal associations in the *D. aegyptiensis* biozone can be assigned to the NP 16 and NP 17 biozones in the peritethyan regions (Deloffre and Genot 1982; Bignot and Neumann 1991; Sztrakos 2000, 2001). The *Discorbis vesicularis* biozone was defined by the first occurrence of the *D. vesicularis* at the base and the last occurrence of *Pseudoclavulina cocoaensis* at the top (Shamah and Helal 1993a). This biozone is represented by 20 m thick in the middle part of the Maadi Formation at the Darbet El-Houity and Geneifa sections. The *D. vesicularis* biozone is considered to be Late Eocene in age. It also includes other foraminiferal species such as *Cibicides proprius* Brotzen, *C. lobatulus* Walker & Jacob, *Globulina gravida* Terquem, *Quinqueloculina carinata* d'Orbigny, *Quinqueloculina impressa* Reuss, *Triloculina enoplostoma* Reuss and *Triloculina trigonula* Lamark.

In summary, the Eocene succession in the study area can be classified into four larger benthic foraminiferal biozones arranged from the base to the top: (1) *A. frumentiformis* biozone

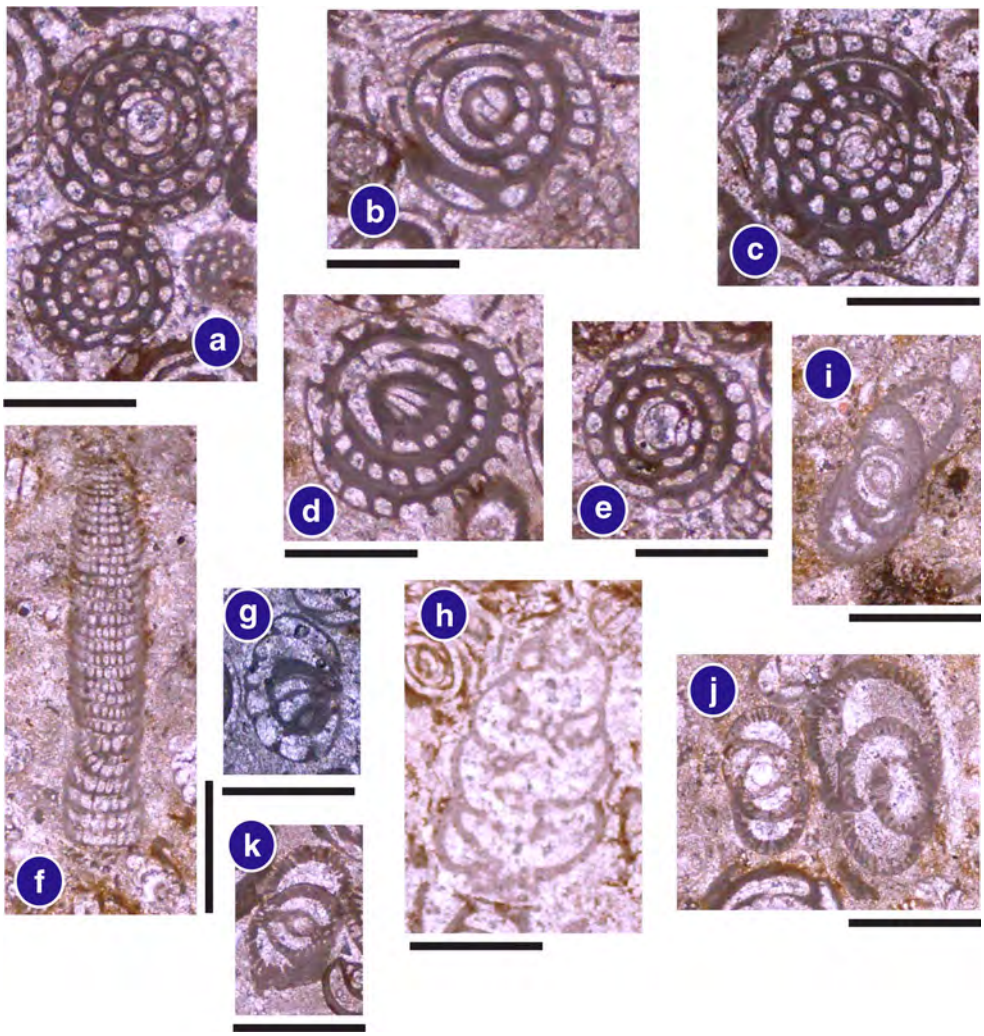

Fig. 8 Photomicrographs showing **a**–**e** *Pseudolacazina schwagerinoides* (Blanckenhorn), Sannor Formation, EGH, SSW, FAN, GEN sections, samples EGH33,34, SSW3,4, FAN7,13,14, GEN18,20,23; **f** *Rhabdorites minima* (Henson), Sannor Fm., SSW, FAN, EGH sections, samples SSW2, EGH12, FAN8; **g** *Peneroplis dusenbury* Henson, Sannor Fm., EGH, SSW sections, samples EGH13, SSW1; **h** *Valvulina* gr. *schwageri* Chapman, Sannor Fm., GEN, SSW sections, samples GEN36, SSW1,2; and **i**–**k** *Planotrillina deserti* Bignot and Strougo, Sannor Fm., SWW section, sample SSW2. *Scale bar*=1 mm

Table 2 Description of the microfacies types and their related depositional environments

MFTs	FA	Description	Occurrences	Depositional environment
1 Lime–mud	FA-4 FA-6	The rocks of this microfacies are thin bedded, chalky limestones. It is composed of micritic matrix, including very rare scattered benthos and algal debris. This micrite is partially neomorphosed into microsparry calcite.	Minia and Sannor formations (EGH, GEN)	Open deep shelf (FZ 3), within euphotic zone and above fair-weather wave base, with moderate to open circulation (Wilson 1975)
2 Alveolinal wacke/packstone (Fig. 10a)	FA-6	It is mainly characterized by *Alveolina frumentiformis* tests (50–60 %) embedded in a micritic matrix that shows a partial neomorphism into microsparry calcite. Other bioclastics (miliolids, orbitolites and algae) are also recorded (20 %). Most allochems are well preserved. Randomly scattered, medium-grained quartz and dolomite rhombs (5 %) are also found in the mictric matrix.	Minia Fm. (EGH, FAN)	Outer shelf lagoons near the back-shoal of the mid-ramp platform (Stefan et al. 2011; Wilson 1975)
3 Miliolida/alveolinal packstone to grainstone	FA-6	It consists mainly of *Alveolina frumentiformis* (50 %) and miliolid (20 %) tests. Other tests of *Idalina* sp., *Biloculina* sp., *Triloculina* sp. and *Orbitolites* sp. (3–5 %) are also recorded. These allochems are embedded in a micrite with some patches of sparry calcite cement. Some miliolid and alveolina tests display partial micritization at their outer rims. Very rare quartz grains and dolomite rhombs were also noticed.	Minia Fm. (EGH, FAN)	Outer shelf lagoons with open circulation (Dill et al. 2007; El-Ayyat 2013)
4 Sandy oyster wacke/packstone	FA-5 FA-6	This microfacies type is characterized by an abundance of oyster shells; most of these shells are well preserved, maintaining its fibrous internal structure. Echinoid plates were also recorded. These allochems are embedded in a micritic matrix including few minute crystals of dolomite. Quartz is fine to medium grained and angular to sub-rounded, showing a wavy extinction.	Maadi Fm. (DEH, EGH, SSW, FAN, GEN)	Inner sheltered lagoon, low energy, well oxygenated and normal salinity (Wilson 1975)
5 Algal wackestone (Fig. 10b)	FA-4	In consists of calcareous algal fragments (40 %) and alveoline tests (less than 3 %) embedded in a micritic matrix with some patches if microsparry calcite. The algae is well oriented parallel to the bedding planes. Ostracods (less than 1 %) and some other bioclastics were also noticed.	Minia Fm. (FAN, EGH)	Light-penetrated photo-synthetic zone on a restricted marine platform (Wilson 1975)
6 Dolomicrite (Fig. 10c)	FA-2 FA-3	The rock of this microfacies is massive, grey, hard dolomite. This microfacies is made up of fine, euhedral to subhedral, equigranular, unzoned dolomite rhombs.	Sannor Fm. (FAN, EGH, GEN)	Intertidal to supratidal zones, lacustrine/palustrine (Tucker and Wright 1990)
7 Miliolida/*Dictyoconus* wacke- to packstone (Fig. 10d)	FA-4	The rocks of this microfacies are greyish white, thick-bedded limestones including gypsum veinlets. This microfacies consists mainly of miliolid tests (*Idalina*, *Quinqueloculina*, *Triloculina*, *Biloculina* and *Pyrgo*) and others such as *Dictyoconus* sp., *Somalina* sp. and *Rhabdorites* sp. All these tests are embedded in a homogeneous micritic matrix with some sparry calcite patches.	Sannor Fm. (GEN, FAN, EGH, SSW)	Sheltered inner lagoons (Geel 2000)
8 Dictyoconus/bryozoa wacke- to packstone	FA-4	It is characterized by abundance of *Dictyoconus aegyptiensis* and several species of Miliolidae. Echinoid spines, algal debris and fine crystalline dolomite rhombs are also shown with	Sannor Fm. (FAN, GEN, EGH)	Inner lagoons characterized by a calm, low-energy and light-penetrated photo-synthetic zone (Hottinger 1997)

Table 2 (continued)

MFTs	FA	Description	Occurrences	Depositional environment
		rare amounts between the biogenic particles. All components are embedded in a microsparritic matrix.		
9 Miliolida grainstone (Fig. 10e, f)	FA-4	The microfacies is made up of different allochemical components embedded in a sparritic groundmass, micritic in parts. The allochems are mainly of miliolids (up to 85 %), represented by *Idalina* sp., *Pseudolacazina* sp., *Quinqueloculina* sp. and *Triliculina* sp. Other benthos like *Planotrillina*, *Dictyoconus* and *Orbitolites* are also recorded forming about 10 % of the framework. Most components are well preserved and their chambers are partially filled by sparite.	Sannor Fm. (EGH, GEN, FAN, SSW)	Protected inner lagoonal environment in the back-ramp setting (Hottinger 1997)
10 Somalina/miliolida pack- to grainstone (Fig. 10g)	FA-4	The rock of this microfacies is greyish white, thick-bedded, bioturbated chalky limestone. This microfacies is composed of allochems represented by *Somalina stefeninii* (up to 40 %), miliolids (8 %), *Orbitolites* sp. (6 %), *Rhabdorites* sp. (5 %), algae (3 %) and *Dictyoconus aegyptiensis* (less than 2 %) cemented by sparry calcite. These allochems are well preserved and their chambers are filled by microsparry calcite.	Sannor Fm. (GEN, FAN, EGH, SSW)	Inner lagoons with restricted conditions (Boukhary and Abdelmalik 1983)
11 Somalina grainstone (Fig. 10h)	FA-4	This microfacies type is characterized by the predominance of *Somalina stefaninii* (up to 45 %) and other benthic oraminifera such as miliolids (15 %), *Dictyoconus* sp. (5 %), bryozoa (0.5 %), echinoids (0.5 %) and algal fragments. All these allochems are well preserved and embedded in a microcrystalline calcitic matrix.	Sannor Fm. (GEN)	Sheltered lagoonal environment in the inner ramp setting (Boukhary and Abdelmalik 1983)
12 Sandy miliolida packstone (Fig. 11a)	FA-5	This microfacies is represented mainly by closely packed miliolids (60 %), *Dictyoconus* sp., (5.0 %), *Rhabdorites* sp., (2.0 %), octracoda and algal debris cemented by microsparry calcite. Sub-rounded, monocrystalline quartz grains are found with about 10 % of the rock volume.	Sannor Fm. (SSW)	Shoal bars with a high clastic input into the inner shelf lagoon from the adjacent lands (Wilson 1975)
13 Sandy molluscan pack- to grainstone	FA-3	This microfacies is made up of allochemical components (70 %) represented mainly by well-sorted, impericated, partially recrystallized molluscan shell fragments (pelecypods and gastropods) within a microsparritic to micritic matrix. Scattered intraclasts and sub-rounded quartz grains are also recorded.	Sannor Fm. (EGH, FAN)	Tidal bars and beaches. Normally above fair-weather wave base (FWWB) and strongly influenced by tidal currents (Wilson 1975)
14 Foraminiferal dololicrite (Fig. 11b–d)	FA-3	The rock of this microfacies is made up to euhedral to subhedral, equigranular, fine crystalline dolomite rhombs (10 %) and about 10 % foraminiferal fossils (*Somalina*, *Dictyoconus* and *Idalina* tests). The dolomite rhombs are zoned displaying a dark core and light outer rims.	Sannor Fm. (GEN)	Paritidal environment (Khalifa 1996; Wanas 2008)
15 Dolomicrite (Fig. 11e)	FA-3	The rock of this microfacies is non-fossiliferous, very hard, dark grey in colour and massive. This microfacies consists mainly of fine crystalline, euhedral to subhedral, equigranular dolomite rhombs. The dolomite rhombs are zoned displaying a dark core and light outer rims.	Sannor Fm. (GEN, EGH, FAN)	Tidal flats in the back-ramp setting (Tucker and Wright 1990)
16 Claystone/siltstone	FA-1	The claystone/siltstone is compact, massive and highly cracked by acicular gypsum. It occurs as interbeds with the limestones and dolostones.	Sannor Fm. (EGH, FAN)	These packages of interbedded claystone and foraminiferal limestone reflect deposition

Table 2 (continued)

MFTs	FA	Description	Occurrences	Depositional environment
				in protected lagoons with restricted circulation (Flügel 2004)
17 Ferruginous–calcareous quartz–arenite (Fig. 11f)	FA-1	This microfacies consists mainly of quartz grains (80 %) with few opaque mineral grains (5 %), cemented by ferruginous and calcareous materials. The quartz grains are monocrystalline, moderately sorted and sub-rounded to rounded. Most of the quartz grains display unit extinction, while few of them show wavy extinction. They also display concavo-convex contacts.	Sannor Fm. (EGH, FAN)	Fluvial channels (Wilson 1975; Flügel 2004)
18 Polymectic conglomerates (Fig. 11g)	FA-1	It is mainly composed of coarse-grained, rounded to sub-rounded, ill-sorted pebbles and cobbles of limestone, dolomite and quartz. The texture is closely packed, cemented by iron oxide materials or by coarse sparritic cement.	Sannor Fm. (EGH, FAN)	Fluvial channels (Wilson 1975; Flügel 2004)
19 Sandy bioclastic wacke/packstone (Fig. 11h)	FA-3	In the field, the rock of this microfacies is yellowish grey, thick-bedded, marly limestone that is highly laden with large-sized oyster shells. This microfacies is formed of poorly sorted fragmented shells of oysters (60 %), together with subordinate bryozoa, echiloid debris and spines, ostracoda and miliolids. These allochemical particles are packed and embedded in a macritic matrix. The main bulk of shell fragments is recrystallized, while some others still retain their fibrous microstructure. Few scattered zoned dolomite rhombs and sub-rounded, medium- to coarse-grained quartz are also found (5 %).	Maadi Fm. (DEH, GEN, EGH, SSW, FAN)	Shallow marine (subtidal shelf), with normal salinity and high energetic conditions (Wilson 1975; Flügel 2004). The detrital grains indicate a high clastic supply
20 Sandy bioclastic packstone	FA-5	The rock of this microfacies is yellowish grey, hard, thick-bedded marly limestone. This microfacies is characterized by the abundance of packed molluscan shell fragments (*Carolia*, oysters, gastropods) forming about (65 %) of the framework. Subordinate ostracods and bryozoan debris, echinoid spines and plates are also recorded. Most bioclastics are recrystallized. Fine- to medium-grained quartz (20 %) and few glauconite grains are also recorded. All these bioclastics are cemented by sparry calcite.	Maadi Fm. (DEH, GEN, EGH, SSW, FAN)	Well-oxygenated shallow subtidal environment under high agitated conditions. The mollusc banks enhance deposition on a winnowed shelf edge (shoal bar), with a susceptibility to subaerial exposure (Wilson 1975; Flügel 2004)
21 Fossiliferous calcareous quartz–arenite	FA-3	It is characterized by yellowish to earthy grey colours, fine- to medium-grained, hard and fossiliferous. It consists mainly of quartz grains (80 %) and poorly sorted shell fragments of oysters, bryozoa, crinoid debris and echinoid plates and spines cemented by dense micrite. Most oyster shells maintain their original fibrous microstructure. The quartz is fine- to medium-grained, moderately sorted and sub-rounded and shows straight extinction.	Maadi Fm. (EGH, DEH)	Subtidal shelf (Flügel 2004)
22 Laminated claystone	FA-4	The claystone is laminated, dark grey, reddish to brownish and blackish in colour and saliferous. It is interbedded with few bands of siltstone.	Maadi Fm. (EGH, FAN, SSW)	Protected lagoons under quiet water conditions (Wilson 1975)

(Late Ypresian), (2) *O. clavata* biozone (Bartonian), (3) *D. aegyptiensis* biozone (Bartonian) and (4) *D. vesicularis* biozone (Priabonian).

Facies analysis and depositional environments

Based on field investigation and thin section analysis, 22 sedimentary microfacies types (MFTs) have been identified in both clastic and carbonate rocks of the studied Eocene succession (Table 2). These microfacies are grouped into six facies associations (FA) corresponding to six depositional environments sited on the inner ramp setting (Fig. 9). Data for facies analysis and its interpretation are based on the Carbonate Ramp Model of Burchette and Wright (1992) describing the inner, mid- and outer parts of platform ramps. The main lithological and micro-textural characteristics of each facies association and its related depositional environments are discussed below:

Floodplain-dominated fluvial facies association: FA-1

Occurrence and description

The FA-1 constitutes the lower part of the Sn_2 at the El-Goza El-Hamra section (Figs. 3 and 12a). It attains a thickness of about 45 m. It consists of conglomerate and pebbly sandstone bodies at the base and siltstone and mudrocks at the top, with erosional lower boundary and fining-upward tendencies. No marine fossils were recorded in this facies association (FA-1). The conglomerates and pebbly sandstone bodies are commonly massive (Fig. 12b), whereas some sandstone bodies exhibit flat stratification and a planar cross-stratification (Fig. 12c). These coarse-grained bodies have an infiltration matrix consisting of

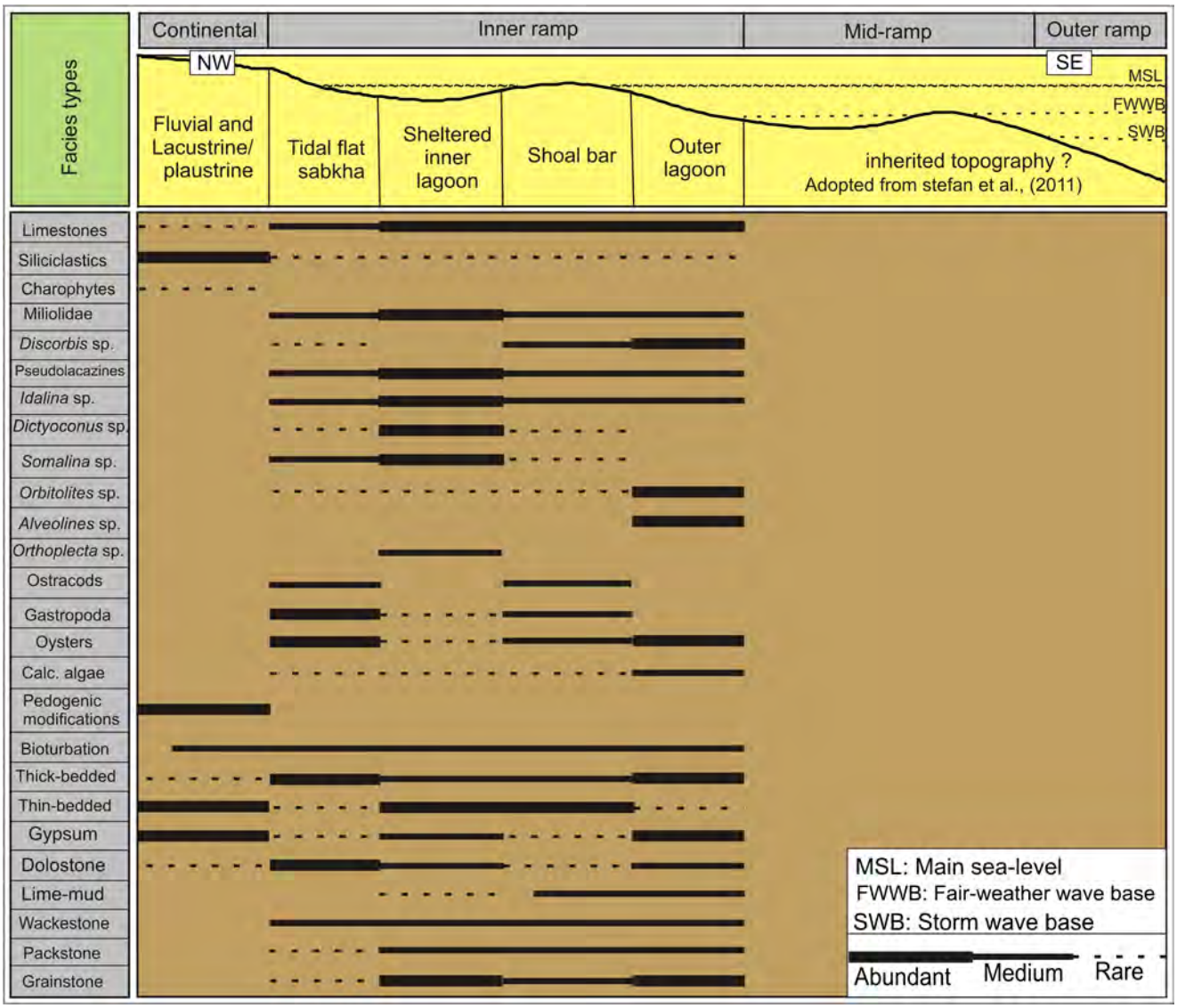

Fig. 9 Sketch showing the depositional model of the Eocene rocks in the Shabrawet area

sand, silt and clay-sized, poorly sorted particles. The fine-grained bodies (siltstone, silty mudrocks and mudrocks) are multi-coloured (white, purple, yellowish-grey, yellowish orange and reddish brown to light brown). This multi-coloured pattern (colour mottling) occurs in both horizontal and vertical strips, as well as in irregular forms (Fig. 12d).

Interpretation

The sedimentological characteristics of the FA-1 point to sedimentation on alluvial plains crossed by fluvial channel, where the coarse load was deposited in relation to the movement of channel bedforms (dunes, transverse bars and longitudinal bars). The fine-grained sediments were deposited in the adjacent floodplains during channel migration (Kraus 1999). As a consequence of channel migration, the finest sediments were subjected to periodic exposure and show evidence of pedogenesis, forming well-expressed soil horizons (Kraus 1999). The pedogenesis is documented by the presence of colour mottling, which could be a result of leaching (light mottles) and precipitation of ferric oxyhydroxides (coloured mottles) (Kraus 1999). The absence of pedogenic features in a coarse-grained channel may be due to rapid sedimentation. On the other hand, the development of pedogenesis in the fine-grained floodplain-dominated deposits indicates that the overbank deposition was quite slow, and after deposition, these sediments were subjected to pedogenic modifications (Marriott and Wright 1993; Kraus and Aslan 1993).

Lacustrine/palustrine facies association: FA-2

Occurrence and description

The FA-2 represents the upper part of the Sn_2 at the El-Goza El-Hamra section (Figs. 3 and 12a). It consists of 10–12 m thick of interbedded fine-grained siliciclastic rocks, marlstone, dolostone and dolomitic limestone. The predominant dolomitic limestone displays a micritic nature, wavy to irregular lamination, brecciation, desiccation cracks and root traces (Fig. 12e). There is no occurrence of marine fossils except for small gastropods associated with rare freshwater plant remains (mainly *charophytes*) that were recorded by Shamah and Helal (1993b) at the El-Goza El-Hamra section.

Interpretation

The absence of marine fossils, the occurrence of freshwater biota (charophytes, ostracods and small gastropods) and the micritic nature of the limestones suggest deposition within a short-lived isolated shallow freshwater pond with low gradient margins (Platt and Wright 1991; Huerta and Armenteros 2005; Wanas and Soliman 2014). Otherwise, charophytes are generally freshwater plants, which can also flourish in brackish water environments (Sim et al. 2006; Soulié-Märsche 2008; Briant et al. 2013; Grosjean and Pittet 2013) with a water depth of less than 10 m (Cohen and Thouin 1987; Garcia 1994; Soulié-Märsche 2008). Therefore, the FA-2 seems to be deposited in an environment of fresh to slightly brackish water with low salinity such as the lake margin (Grosjean and Pittet 2013; Wanas and Soliman 2014). In addition, the prevalence of desiccation cracks, root traces and brecciation within the dolomitic limestones is an indicator of their subjection to subaerial exposure and pedogenic modifications during semi-arid to sub-humid periods. These features are common in palustrine limestones (Platt and Wright 1992; Alonso-Zarza and Wright 2010; Wanas and Soliman 2014).

Tidal flat facies association: FA-3

Occurrence and description

The FA-3 is dominated in the carbonate beds of the Sn_2 (Fig. 3). Prevailing carbonate rock types are homogeneous, yellowish grey in colour with very restricted and delicate fauna. In addition, this facies occurs in the upper unit of the Maadi Formation (Fig. 3), where it consists of cross-bedded sandstones and siltstones. Microscopically, the carbonate beds include dolomicrite, dolosparite and dolomitic lime–mudstone microfacies (Table 2; Figs. 10c and 11e). This microfacies is composed of dolomite rhombs, which can be differentiated into two types. The first type (80 % of the rock volume) is represented by fine crystalline rhombs ranging from 20 to 50 μm. The matrix is formed of lime–mudstone that has few gypsum-filled pores. Most of the dolomite rhombs show hypidiotopic fabric with equigranular texture. They are unzoned but have cloudy cores with clear outer rims. The second type of dolomite (30–40 % by volume) is less abundant. The dolomite rhombs range in size from 90 to 130 μm and are idiotopic to hypidiotopic in fabric with unequigranular texture. Some rhombs show zoning that occurs as brownish yellow cores with thin clear outer rims.

Interpretation

The observed fine crystalline, unzoned dolomite rhombs with very restricted fauna (the first type) are closely similar to those recorded in ancient tidal flats by many workers. Out of them, Khalifa (1981) described fine-grained dolomite rhombs in the Lower Eocene and attributed them to contemporaneous dolomitization of lime–mud in supratidal flats. According to Khalifa (1996), Wanas (2008) and El-Ayyat (2013), the occurrence of fine crystalline dolomite in the platform carbonate indicates

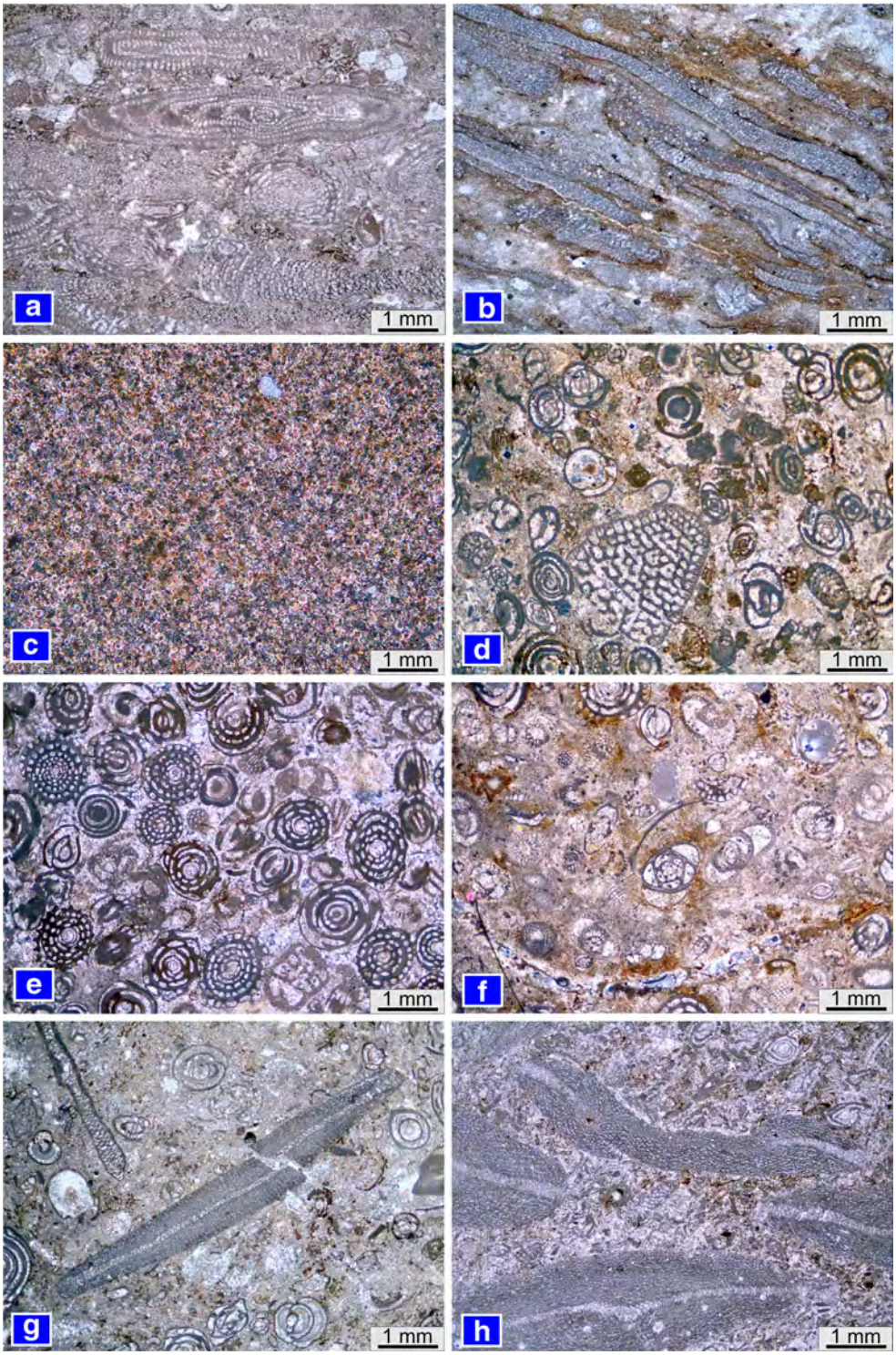

Fig. 10 Photomicrographs showing **a** alveolinal wacke/packstone, Minia Fm., EGH, FAN sections, samples EGH1-4, FAN1-4; **b** algal wackestone, Minia Fm., EGH, FAN sections, samples EGH5, FAN5; **c** dolomicrite, Minia and Sannor formations, EGH, FAN sections, samples EGH16, FAN6; **d** miliolida/dictyoconus wacke- to packstone, Sannor Fm., GEN, FAN, EGH, SSW sections, samples EGH11-14, GEN23-25, FAN12-14, SSW3; **e**, **f** miliolida grainstone, Sannor Fm., GEN, EGH, FAN, SSW sections, samples GEN30-32, EGH33-34; **g** *Somalina*/miliolida pack- to grainstone, Sannor Fm., GEN, FAN, EGH sections, samples EGH22-25, GEN28-29; and **h** *Somalina* grainstone, Sannor Fm., GEN section, samples GEN27-31

peritidal (upper intertidal–supratidal) carbonates that were formed during sea level fall. On the other hand, Tucker and Wright (1990) attributed the formation of the fine crystalline dolomite associated with gypsum crystal-filled pores to intensive evaporation of marine water in a supratidal zone during a short period of sea level fall, and a contemporaneous replacement of a previously deposited lime–mudstone. Similar cases were also recorded in the tidal flat limestone of the Illinois Basin (Choquette and Steinen 1980); southwest Andros Island (Gebelein et al. 1980); Sinai Peninsula, Egypt (Wanas 2008); and Farafra Depression, Egypt (El-Ayyat 2013). The observed coarse-

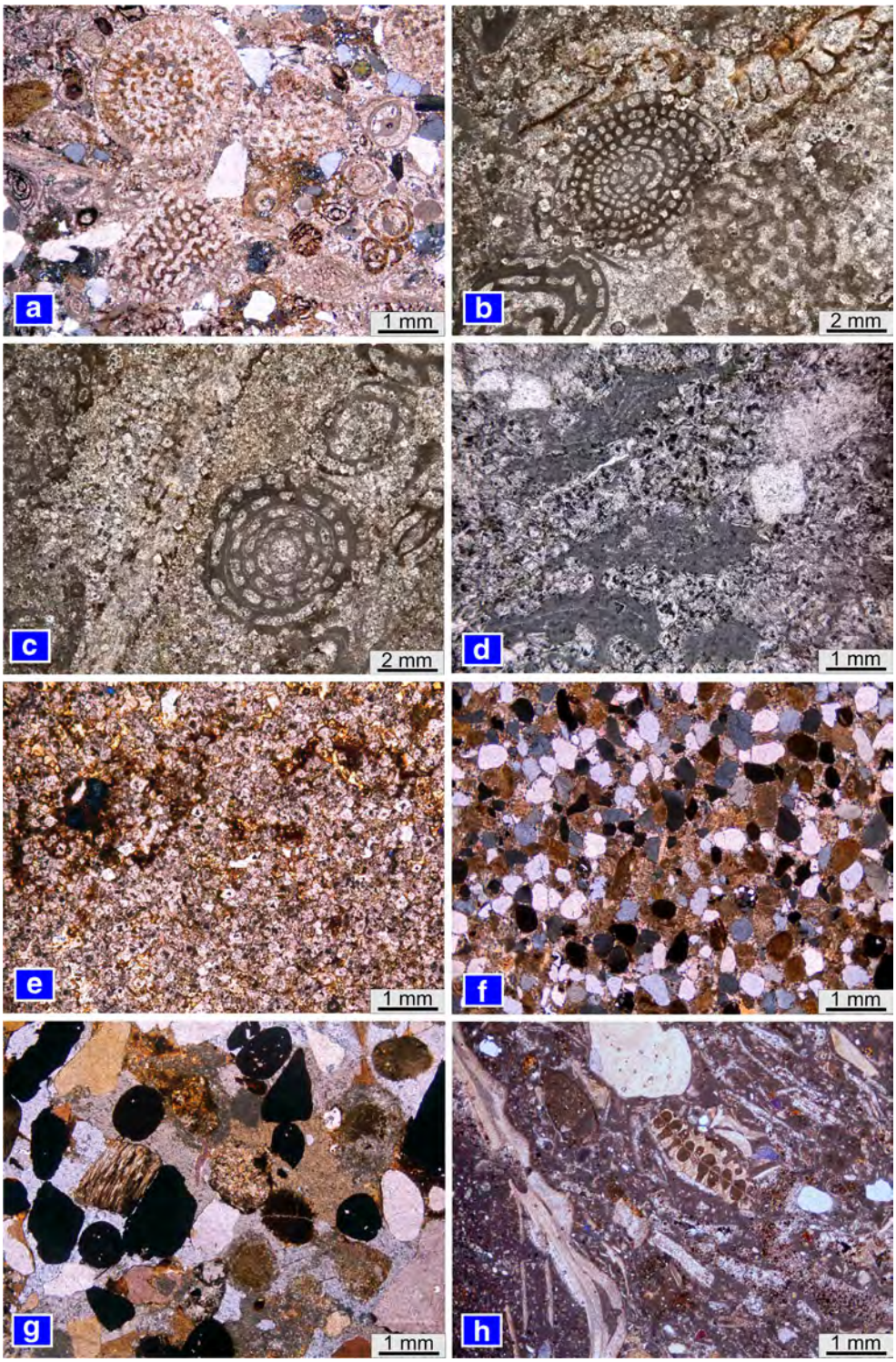

Fig. 11 Photomicrographs showing **a** sandy miliolida packstone, Sannor Fm., SSW section, samples SSW4,5; **b–d** foraminiferal dolosparite, Sannor Fm., GEN section, samples GEN1,3; **e** dolosparite, Sannor Fm., GEN, EGH, FAN sections, samples GEN8,15; **f** ferruginous–calcareous quartz–arenite, Sannor Fm., EGH, FAN sections, samples EGH-P1,3,4; **g** polymectic conglomerates, Sannor Fm., EGH, FAN sections, samples EGH-P2; and **h** sandy bioclastic wacke/packstone, Maadi Fm., DEH, EGH, FAN, GEN, SSW sections, samples DEH8-10, SSW6-7, EGH35-36

zoned dolomite rhombs with a faunal restriction (the second type) are probably a late diagenetic product of the previously formed fine dolomite during burial (Tucker and Wright 1990). The cross-bedded sandstone and siltstones of the upper unit of the Maadi Formation most probably indicate deposition close to the shore.

Restricted inner lagoon facies association: FA-4

Occurrence and description

The FA-4 dominantly occurs in the Sn_1 and the uppermost part of the Sn_3 at the El-Goza El-Hamra, Fanara and Geneifa

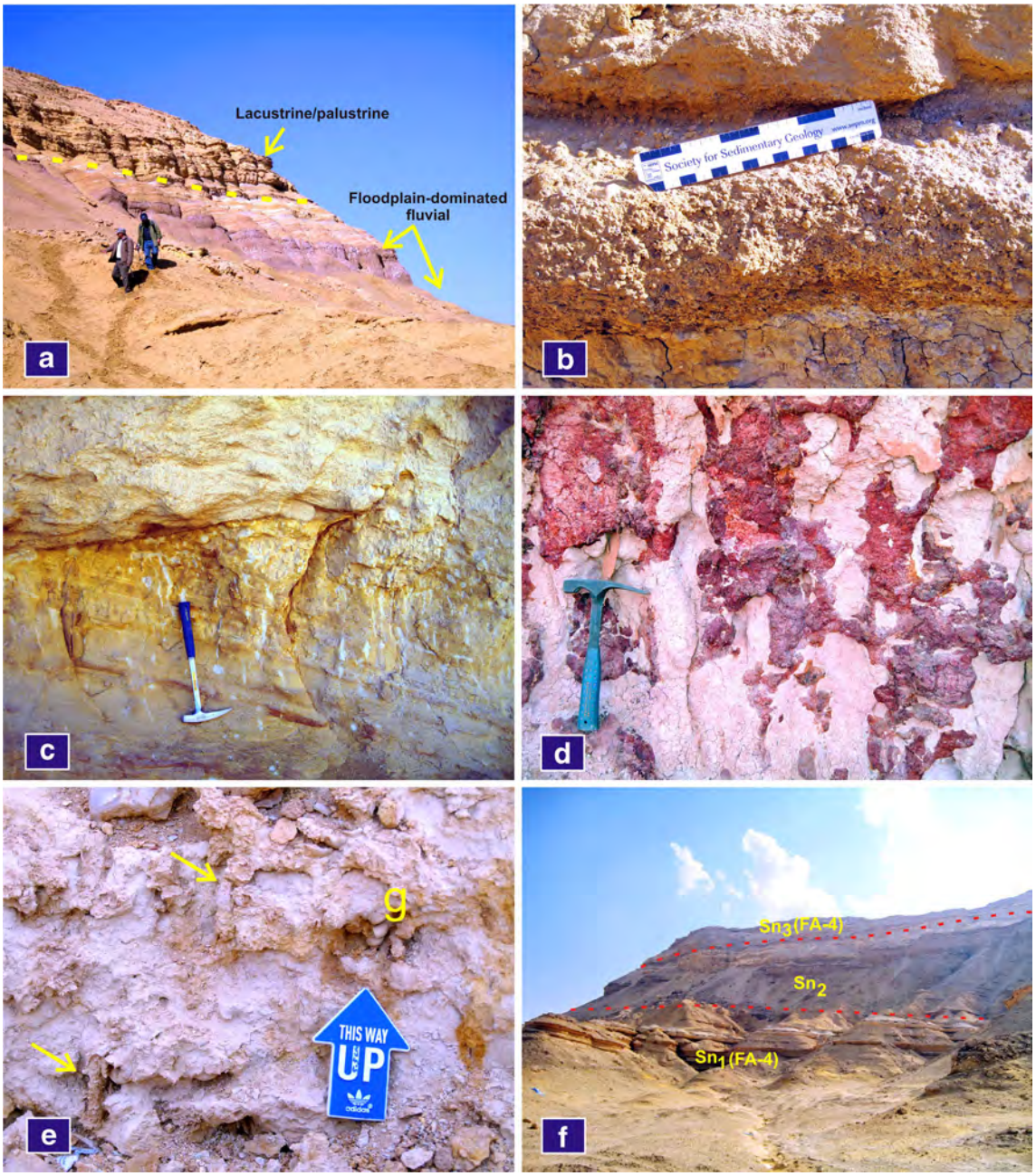

Fig. 12 Field photographs showing **a** floodplain-dominated fluvial (FA-1) overlain by lacustrine/palustrine facies association (FA-2), EGH section; **b** conglomerate interbeds within the FA-1, consisting mainly of quartz and dolomite pebbles and cobbles, embedded in a sand matrix, EGH section; **c** cross-bedded silty sandstone characterizes the lower part of the FA-1, displaying colour mottling, EGH section; **d** red and grey colour mottling in siltstone due to leaching (light mottles) and precipitation of ferric oxyhydroxides; **e** root traces (*yellow arrows*) and gastropod (*g*) fossils within the rocks of the FA-2, EGH section; and **f** crudely bedded limestone alternated with yellowish marly limestone and claystone of the FA-4, EGH section

sections (Fig. 3). The rocks of this facies association consist of alternation of crudely bedded limestone with bands of yellowish marly limestone, marlstone and silty to sandy marlstone (Fig. 12f). These carbonate beds occasionally intercalated with yellowish green shales. Bioturbation is the most common sedimentary structure. The rocks of the FA-4 are also represented by the gypsiferous shales and the sandy shelly (*Ostrea*-rich) wacke/packstone facies of the lower unit of the Maadi Formation. Petrographically, the dominant microfacies are wackestones and wacke- to packstones (Table 2; Fig. 10d–h). Faunal content includes miliolids, *S. stefaninii*, *D. aegyptiensis*, *I. cuvillieri*, *P. schwagerinoides*, *R. minima* and calcareous algae, in addition to few small textulariid foforams. Pelloids and ostracods of different shapes and nearly the

same size are scattered in the micrite matrix. The miliolids, *I. cuvillieri* and *P. schwagerinoides* are the dominant fossil contents. Based on the abundance of the faunal content, different sub-microfacies were described (Table 2). Most of the fauna show micritization and/or micrite coating and the micrite matrix displays a patchy neomorphism.

Interpretation

The presence of miliolids and/or small textulariids and the absence of high diversity of fossils typically indicate restricted shallow quiet water, probably a restricted lagoon or sheltered bays with high salinity (Hottinger 1997). The occurrence of peloids and heavy micritized skeletal particles in the micrite matrix suggests deposition in a protected quiet water zone (restricted lagoon) where responsible microbial boring mats (endolithic algae, bacteria, or fungi) prevailed (Tucker and Wright 1990). Geel (2000) mentioned that miliolids prefer low turbulence and soft substrates and when abundant indicate restricted lagoon. Buxton and Pedley (1989) and Hallock and Glenn (1986) stated that abundant miliolids and ostracods characterize the protected embayments in the Tethyan Tertiary carbonate inner ramps. The presence of peloids (micritized grains) indicates shallow marine-protected water with a low-energy, back-bank lagoonal environment, where the burrowing endolithic algae are more active (Tucker and Wright 1990). *S. stefaninii*, *D. aegyptiensis*, *I. cuvillieri*, *P. schwagerinoides*, and *Rhabdorites* wacke/packstones were also recorded in sheltered lagoon environments by Sallam et al. (2015). These microfacies associations are equivalent to SMF 9/FZ 8 of Wilson (1975), which suggests deposition in shallow restricted lagoons of a low-energy environment. The FA-4 is closely similar to that described in the restricted inner lagoon carbonates of the Eocene rocks in different localities in Egypt (Stefan et al. 2011; El-Ayyat 2013; Sallam et al. 2015). In addition, the gypsifeous shale beds and the sandy shelly (*Ostrea*-rich) wacke/packstone facies in the lower unit of the Maadi Formation may reflect sedimentation in a restricted inner lagoon of low-energy, well-oxygenated, normal saline water.

Shoal bar facies association: FA-5

Occurrence and distribution

The rocks of the FA-5 constitute the uppermost part of the Sn_3 and the Maadi Formation at all the studied sections (Fig. 3). These rocks are thick-bedded, bioturbated, greyish white limestones that show a bird's eye structure. They are intercalated with vuggy dolomite beds. Microscopically, the FA-5 consists of mud-free, well-sorted, and medium to coarse skeletal grainstones. This facies includes several sub-microfacies such as *Pseudolacuzina*, miliolids and *Idalina* grainstones (Table 2; Fig. 10d, e). The skeletal allochems form about 60–70 % of the rock volume. The cement between allochems is mainly sparry calcite. In addition, this facies association contains quartz grains (5–7 %) and bioclasts (5–10 %). The rocks of the FA-5 in the uppermost part of the Maadi Formation are represented mainly by the sandy limestones rich in *C. placunoides* shells.

Interpretation

The common sparry cement and the good sorting of the components (allochems) in limestones indicate high hydrodynamic conditions and reworking (Dunham 1962). This facies is closely similar to the winnowed platform edge facies of Wilson (1975) and high-energy, well-oxygenated facies of Flügel (1982, 2004). The occurrence of quartz grains and bioclasts in this grainstone facies could be derived from periodic reworking of sediments in extremely shallow water environments with restricted sedimentation (Dunham 1962). Also, the accumulation of *C. placunoides* shells in the sandy limestones of the upper unit of the Maadi Formation may reflect deposition in brackish water near the shore (Carbonel and Pujos 1981). This facies can be deposited in a winnowed platform edge (shoal bar) above the wave base, within the euphotic zone, and highly affected by wave action. The FA-5 is equivalent to SMF 11, 12 and FZ 6 of Wilson (1975) and Flügel (1982, 2004).

Outer lagoon with open circulation facies association: FA-6

Occurrence and description

The FA-6 represents the Minia Formation in the El-Goza El-Hamra, Fanara and Geneifa sections (Fig. 3). It crops out as white, thick-bedded and chalky alveolinal limestones intercalated with few thin bands of gypsum and gypsiferous shale. It displays a cyclic manner forming packages of 5.0, 26 and 9.0 m thick at the Geneifa, Fanara and El-Goza El-Hamra sections, respectively. Petrographically, the dominant recorded microfacies are the lime–mudstone, wackestones, wacke- to packstone and packstones (Table 2; Fig. 10a). Faunal contents are represented by *A. frumentiformis*, *Orbitolites complanatus* and miliolids. Tests of ostracods and benthic forams also occur. *A. frumentiformis* tests are the main fossil content (50–60 %). Most of these fossils are well preserved. These fossils are embedded in a micritic groundmass that is showing a patchy aggrading neomorphism into microsparry calcite.

Interpretation

Alveolina sp. and *Orbitolites* sp. assemblage illuminates in low-turbulence, shallow water marine environments with

open circulation behind a barrier at the distal part of an inner ramp (outer lagoon) (Dill et al. 2007; Stefan et al. 2011; El-Ayyat 2013). The dominance of matrix-supported facies (lime–mudstone, wackestone and packstone) with alveolina and miliolid tests indicates a deposition quite similar to intermittently water conditions (Stefan et al. 2011). Wilson (1975) mentioned that alveolinal wackestone represents shallow subtidal quiet water with open circulation, near the backshoal of the mid-ramp platform (outer shelf lagoon). The FA-6 is equivalent to FZ 7 of Wilson (1975).

Sequence stratigraphy

The sequence stratigraphic terminologies of Van Wagoner et al. (1988), Sarg (1988) and Handford and Loucks (1993), supplemented by modern concepts of Friedman and Sanders (2000), Schlager (2005) and Catuneanu (2006), have been applied in this study. In this study, attention was focused on the determination of surfaces indicating sub-aerial exposures, hardgrounds and abrupt facies changes, which could help in recognition of sequence stratigraphic surfaces and boundaries in both clastic and carbonate successions. The facies distribution and their vertical stacking pattern permit the identification of systems tracts and depositional sequences. The sequence stratigraphic elements are discussed below:

Sequence boundaries

Sequence boundaries in the present study were defined primarily on the basis of evidence for subaerial exposure. Four main sequence boundaries were recognized in the studied sections. These are SB-1, SB-2, SB-3 and SB-4. They are noticed where conglomerate, palaeosol and/or crystalline calcite beds occurred. The SB-1 lies between the Upper Cretaceous–Lower Tertiary Maghra El-Bahari Formation and its overlying Sn_3 at the South Shabrawet West section. It also occurs between the Maghra El-Bahari Formation and its overlying Upper Eocene Maadi Formation at the Darbet El-Houity section. This sequence boundary (SB-1) is delineated by the presence of more or less 6.0 m thick of conglomerates and palaeosol interbeds. The SB-2 occurs between the outer lagoonal carbonate deposits of the Minia Formation and its overlying restricted lagoonal carbonates of the Sn_1 (Fig. 3). At the El-Goza El-Hamra section, the SB-2 is determined due to the occurrence of a sugary crystalline bed of gypsum (45 cm thick) at the base, followed by 4.0 m reworked limestone and duricrust (20 cm thick) and topped by 0.5 m conglomerate mainly of limestone and dolomite pebbles, embedded in a clayey sand matrix. On the other hand, the SB-2 at the Geneifa section is marked by the occurrence of a freshwater crystalline calcite bed (2.0 m thick) between the Minia Formation and the Sn_1 (Fig. 3). The SB-3, at the El-Goza El-Hamra section, occurs between the restricted lagoonal carbonates of the Sn_1 and its overlying continental deposits of the Sn_2 (Fig. 3). Otherwise, at the Geneifa section, the SB-3 is marked by an abrupt transition from restricted lagoonal chalky limestones of the Sn_1 into tidal flat dolomites of the Sn_2. The SB-4 occurs between the lagoonal deposits of the Maadi Formation and its overlying fluviatile rocks (the Gebel Ahmer Formation) of Oligocene age (Fig. 3).

Transgressive surfaces

The transgressive surface (TS) is recognized where there is facies indicating a relative sea level rise above the facies of a sea level fall. In the present study, the first TS is marked at the beginning of the outer lagoon facies of the Sn_1 (Fig. 3). The second TS is recorded directly above the continental deposits (floodplain-dominated fluvial and lacustrine facies) of the Sn_2 and directly below the inner lagoonal deposits of the Sn_3 (Fig. 3).

Systems tract

Systems tract is a package of transgressive (retrogradational) and/or regressive (aggradational and progradational) sedimentary facies. In the present study, three systems tracts including lowstand systems tract (LST), transgressive systems tract (TST) and highstand systems tract (HST) were recognized (Fig. 3). The LST is a progradational facies. It is recorded in the studied area by the floodplain-dominated fluvial, lacustrine and tidal flat facies of the Sn_2, which indicate a relative sea level fall. The TST is a retrogradational facies. It is recognized where there is a relative sea level rise. The TST characterizes the outer lagoonal facies of the Minia Formation, the restricted inner lagoonal facies of the Sn_1 and the upper part of the Sn_3 and the lower part of the Maadi Formation. These facies indicate the maximum relative sea level rises in the study area. The HST is aggradational facies. It is recognized by the shoal bar and tidal flat facies of the upper part of the Maadi Formation. Such facies indicates a relative sea level highstand above the maximum relative sea level rise of the TST facies.

Depositional sequences

A depositional sequence is a stratigraphic unit composed of a relatively conformable succession of genetically related strata, bounded at its top and base by unconformities or their correlative conformities (Vail et al. 1977). On the basis of their stratigraphic setting, facies changes and sequence boundaries and surfaces, the studied Eocene rocks (the Minia, Sannor and

Maadi formations) display the occurrence of three depositional sequences formed in response to relative sea level changes (Fig. 13).

Depositional sequence-1

The depositional sequence-1 characterizes the beds of the Minia Formation. It is bounded by two sequence boundaries. The lower (SB-1) is delineated by the occurrence of angular unconformity surface between the Minia Formation and its underlying inclined Cretaceous strata, whereas the upper sequence boundary (SB-2) is marked by the occurrence of a disconformity between the Minia Formation and its overlying Sn_1. The depositional sequence-1 comprises a TST of retrogradational facies of the Minia Formation (Fig. 3). The retrogradational package consists of outer lagoon facies which marks a relative sea level rise.

Depositional sequence-2

The depositional sequence-2 represents the Sn_1 and it is bounded by two sequence boundaries (SB-2 and SB-3). The SB-2 is discussed above, whereas the SB-3 is marked by the conglomerate beds between the Sn_1 and Sn_2. The depositional sequence-2 includes a TST. This TST package is represented by restricted inner lagoon facies of the Sn_1 (Fig. 3), which marks sea level rise above the SB-2.

Depositional sequence-3

The depositional sequence-3 makes up the Sn_2, Sn_3 and the Maadi Formation (Fig. 3). It is bounded by a lower sequence boundary (SB-3) and an upper sequence boundary (SB-4) (Fig. 3). This depositional sequence is made up of LST, TST and HST. The LST is represented by continental deposits (floodplain-dominated fluvial and lacustrine facies) at the El-

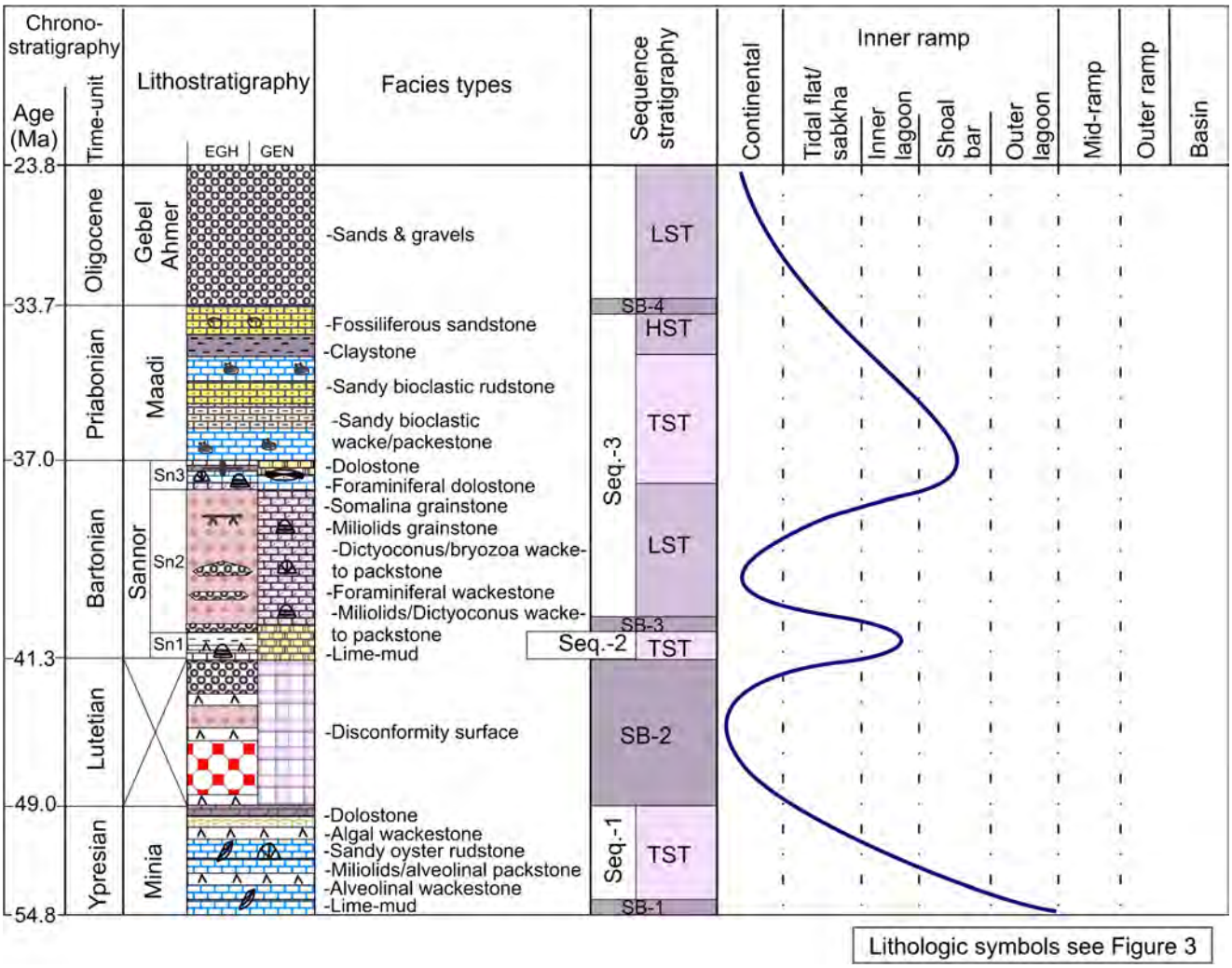

Fig. 13 Suggested sea level curve during the Eocene in the study area. Lithologic symbols, see Fig. 3

Goza El-Hamra and Fanara sections, whereas at the Geneifa section, the LST comprises tidal flat facies. The TST are recorded in all the studied sections. It includes the restricted inner lagoon facies of the lower part of the Maadi Formation and the Sn_3 (Fig. 3). The HST comprises the tidal flat and shoal bar facies of the upper part of the Maadi Formation (Fig. 3). The cyclic sequence of continental deposits, shallow marine deposits (shoal bar facies) and relatively deeper marine deposits (outer and inner lagoon facies) indicates a cyclic sea level rise and fall (Fig. 13).

Discussion

The Cretaceous/Eocene contact in the studied area is unconformable including many stratigraphic gaps that differ in their magnitudes. At the El-Goza El-Hamra section, the inclined Upper Cretaceous strata (dip angles 40°–55°) are overlain by the nearly horizontal Eocene beds (dip angles 6°–10°). At the South Shabrawet West section, the Palaeocene, Lower Eocene and Lutetian rocks are absent due to an angular unconformity separating the inclined strata of the Maghara El-Bahari Formation (Late Cretaceous–Early Tertiary) from the overlying locally folded Bartonian Sannor beds, which may indicate a highly unstable and seismic area reflected in the accentuation of the structural folds along the Syrian Arc System. At the Darbet El-Houity section, the magnitude of the unconformity between the Cretaceous and Eocene gets more wide, since the conglomerate and palaeosol beds of the Maghra El-Bahari Formation are unconformably overlain by the Upper Eocene Maadi Formation.

The studied Eocene rocks were mostly deposited over a shallow marine platform with various depths and energetic conditions, extending in North Egypt along the southern margin of the Tethys. During the late Early Eocene (Late Ypresian), the Shabrawet area was transgressed by the Neo-Tethys and the Minia Formation (mostly thick-bedded algal/alveolinal wacke/packstones) was deposited in outer lagoons and shallow marine environments. The top part of the Minia Formation (of Late Ypresian age) is graded into marly limestone with shale intercalations including considerable gypsum veins and pockets, which may reflect more evaporitic conditions in intertidal and supratidal zones. This suggests that a relative sea level fall occurred during the Late Ypresian age (Fig. 13). This is in agreement with the sea level curve of Haq et al. (1988).

The active block faulting in North Egypt is documented by rising and falling of many structural blocks, which resulted in the presence of the Lutetian rocks in some stratigraphic sections and their missing in others (Said 1990). In the studied sections, there was a missing of Lutetian rocks. These are represented by the occurrence of unconformities. At both the El-Goza El-Hamra and Fanara sections, the unconformity is indicated by the presence of 4.0 m thick of yellowish grey and reddish reworked limestone, duricrust (0.2 m thick) and gypsum deposits, ended by about 0.5 m conglomerate bed. At the Geneifa section, the unconformity is indicated by the occurrence of about 2.0 m thick blocky calcite bed at the base of the section. The palaeosol, gypsum, conglomerate and calcite suggest a major shift in sedimentation, most probably related to the epeirogenic uplift of the area from the close of the Early Eocene up to the late Middle Eocene. The uplift and subsidence movements most probably echoed the Lutetian Pyrenean–Atlasic event: the collision of Africa and Europe plates (ca. 40 Ma) (Guiraud 1986), in response to the opening of the Central Atlantic Ocean (Ziegler 1990; Ziegler et al. 2001; Fairhead et al. 2003). A major NW–SE faulting phase occurred during the Lutetian, associated with a major unconformity during this time span.

By the advent of the Bartonian, the Shabrawet area was subjected to a shallow sea transgression that covered large areas in the NE Desert and Cairo–Suez district. This transgressive phase led to the deposition of a thick carbonate sequence (the lower unit Sn_1 of the Sannor Formation) in a shallow marine environment, most probably sheltered lagoons interrupted by tectonic uplift and semi-arid climate during the late Middle Eocene. During the mid-Bartonian, the northern part of the study area was affected by faulting, uplifting and sub-aerial exposure to arid to semi-arid climatic conditions that most probably was controlled by the episodic rejuvenation of the Syrian Arc folding that affected the area since the Early Cretaceous. In the studied area, this is well expressed in the development of ca. 60-m-thick continental deposits of the Sn_2 at the El-Goza El-Hamra and Fanara sections. These continental deposits are mainly floodplain-dominated fluvial and lacustrine deposits that were subjected to pedogenic modifications. Southward of the study area (at Gebel Geneifa), these continental deposits were replaced by tidal flat dolomite and dolomitic limestones. A new incursion of shallow sea took place in the late Bartonian and led to the deposition of a thick carbonate sequence of the Sn_3 of the Sannor Formation. The rise in sea level in the late Bartonian is also recorded from the Bartonian rocks in several Arab countries (Boukhary et al. 2006).

The last phase in the Eocene deposits occurred during the Priabonian, in which there was a gradual withdrawal of the Neo-Tethys northward off the Egyptian land that led to deposition of thick-bedded, mollusc-rich siliciclastic-carbonate rocks of the Maadi Formation in the area under study. The deposition of the rocks of the Maadi Formation was mainly structurally controlled, hence the variations in thickness and distribution of its rocks. The sandy mollusc packstones of the Maadi Formation suggest deposition in a tidal, nearshore environment with storm/current influence during the concentration of the oyster shells. The intercalated *C. placunoides*, gastropod and oyster banks within the Maadi Formation most

probably reflect deposition in a winnowed inner shelf edge or in marine shoal under brackish water conditions (Carbonel and Pujos 1981). The presence of much terrigenous clastic components (e.g. sand and clay) in the Maadi Formation indicates that the inner shelf was usually subjected to a high input of siliciclastic sediments derived through some channels from the surrounding areas.

The northward withdrawal of the Tethys off Egypt continued in the Oligocene. East Egypt was uplifted during this time, and many river systems running generally in the E–W direction were developed (Said 1990; Issawi et al. 2009). As a result, fluviatile varicoloured sands and gravels rich in silicified wood were laid down in the area under study during Oligocene time. These Oligocene deposits disconformably overlie the Upper Eocene Maadi Formation and disconformably underlie the Miocene marine beds, and can be correlated with the Gebel Ahmer Formation found east of Cairo.

From the foregoing discussion, it is noticed that there are lateral and vertical changes in the environments of deposition of the Eocene rocks. This could suggest that the studied Eocene rocks were deposited in a tectonically active area that was affected by transgression and regression of Neo-Tethys in Egypt. Such tectonic activity is mostly related to the Syrian Arc System (Krenkel 1925–1938) that was renewed and enlarged several times during the Late Cretaceous up to the Neogene (Moustafa and Khalil 1989).

Conclusions

The present work deals with the study of stratigraphy, facies analyses and sequence stratigraphy of the exposed Eocene rocks at the Shabrawet area (north Eastern Desert, Egypt). It is achieved by field observations and petrographic investigations of the Eocene rocks. There, the Eocene succession includes three lithostratigraphic units. These units are, from the base to the top, the Minia Formation (Late Ypresian), the Sannor Formation (Bartonian) and the Maadi Formation (Priabonian). Facies analysis of the examined Eocene rocks helped in the recognition of 22 carbonate and silisiclastic microfacies types. The carbonate microfacies include lime–mud, alveolinal wacke- to packstone, miliolida/alveolinal/dictyoconus pack- to grainstone, sandy oyster wacke/packstone, algal packestone, sandy molluscan pack- to grainstone, dolomicrite and dolosparite. The siliciclastic facies are claystone/siltstone, ferruginous/calcareous quartz arenite and polymectic conglomerates. These microfacies types are grouped into six facies associations, equivalent to six depositional environments sited on an inner ramp setting. These depositional environments include the floodplain-dominated fluvial, lacustrine/palustrine, tidal flat, restricted inner lagoon, shoal bar and outer lagoon with open circulation. A suitable depositional model of the studied Eocene rocks is constructed.

Biostratigraphically, four benthic larger foraminiferal biozones were recognized in the studied Eocene rocks. These are, from the base to the top, (1) *A. frumentiformis* biozone (Late Ypresian), (2) *O. clavata* biozone (Bartonian), (3) *D. aegyptiensis* biozone (Bartonian) and (4) *D. vesicularis* biozone (Priabonian).

The studied Eocene rocks have been subdivided into three superimposed depositional sequences. These sequences were formed in response to the eustatic sea level change during the Eocene. Each sequence comprises retrogradational (TST) and aggradational (HST) to progradational (LST) packages of sedimentary facies. The retrogradational package is represented by the outer lagoon and the restricted inner lagoon facies, the aggradational is manifested by the shoal bar and tidal flat facies, whereas the progradational facies tract is reflected in the occurrences of fluvial and lacustrine/palustrine facies. In the study area, it is noticed that there are abrupt lateral and vertical changes in the depositional environments of the Eocene rocks, between shallow marine and continental environments. Also, the occurrence of many unconformities within the Eocene platform succession and its evolution suggest that the sedimentation has been influenced strongly by the tectonic activity rejuvenated episodically along the Syrian Arc Fold Belt.

Acknowledgments The authors are very grateful to Dr. Issawi B., former Director of the Geological Survey and Mining Authority of Egypt, for reviewing the manuscript and valuable discussion that greatly benefited this work. Prof. Boukhary M., Ain Shams University, is greatly acknowledged for his help in the identification of the larger benthic foraminifers and his contribution in the biostratigraphic study. Dr. Haggag W., Benha University, is also acknowledged for being helpful and for being an amicable field assistant. Many thanks are due to two anonymous reviewers for their critical revision of the manuscript. Special thanks are also due to Prof. Abdullah M. Al-Amri (Editor-in-Chief) for his editorial support.

References

Abu El-Ghar MS (2007) Eocene stratigraphy, facies, sequences and depositional history in Shabrawet area, North of Suez, Eastern Desert, Egypt. ISESCO 3:23–42

Al-Ahwani MM (1982) Geological and sedimentological studies of Gebel Shabrawet area, Suez Canal District, Egypt. Ann Geol Surv Egypt 12:305–379

Alonso-Zarza AM, Wright VP (2010) Palustrine carbonates. In: Alonso-Zarza AM, Tanner LH (eds) Carbonates in continental settings: facies, environments, and processes. Developments in sedimentology, vol 61. Elsevier, Amsterdam, pp 103–131

Beadnell HJ (1905) The topography and geology of the Fayium province of Egypt. Geol. Surv. Egypt, 101p

Bignot G, Neumann M (1991) Les «grands» Foraminifères du Crétacé terminal et du Paléogène du Nord-Ouest européen. Recensement et extensions chronologiques. Bull Inf Géol Bassin Paris 28/2:13–29

Boukhary MA, Abdelmalik W (1983) Revision of the stratigraphy of the Eocene deposits in Egypt. N Jb Geol Palaont Mh Stuttgart 6:321–337

Boukhary MA, Decrouez D, El Safori YA (2006) *Somalina stefaninii* n.sp., a new species of large foraminifera from the Dammam Formation (Lutetian) of Gebel Hafit, United Arab Emirates. Geol Croatica, Zagreb 59(2):99–107

Briant RM, Bates MR, Boreham S, Coope GR, Schepper SD, Field MH, Weban-Smith FF, Whittaker JE (2013) Paleoenvironmental reconstruction from a decalcified interglacial sequence in the former Solent River system at St Leonard's Farm, Hampshire, England. Quat Newsl 130:23–38

Burchette TP, Wright VP (1992) Carbonate ramp depositional systems. Sediment Geol 79:3–57

Buxton MW, Pedley HM (1989) A standardized model for Tethyan Tertiary carbonate ramps. J Geol Soc 146:746–748

Carbonel P, Pujos M (1981) Comportment des microfaunes benthiques en milieu lagunaire. Actis du Premier Congres Natl. Sci. de la Terre (Tunis), pp. 127–140

Catuneanu O (2006) Principles of sequence stratigraphy. Elsevier, New York, 386p

Choquette PW, Steinen RP (1980) Mississippian non-supratidal dolomite Ste. Genevieve Limestone, Illinois Basin: evidence for mixed-water dolomitization. In: Zenger DH, Dunham JB, Ethington RH (eds) Concepts and models of dolomitization, Spec. Publ. Soc. Econ. Paleont. Miner., 28: 168–196

Cohen AS, Thouin C (1987) Nearshore carbonate deposits in Lake Tanganyika. Geology 15:414–418

Deloffre R, Genot P (1982) Les algues Dasyeladales du Cénozoïque. Bull. Centres Rech., Explor. Prod. Elf Aquitaine. Pau. mém. 4, 247p

Dill HG, Wehner H, Kus J, Botz R, Berner Z, Stüben D, Al-Sayigh A (2007) The Eocene Rusayl formation, Oman, carbonaceous rocks in calcareous shelf sediments: environment of deposition, alteration and hydrocarbon potential. Int J Coal Geol 72:89–123

Dunham RJ (1962) Classification of carbonate rocks according to depositional texture. In: Ham WE (ed) Classification of carbonate rocks. Tulsa, Okla. A.A.P.G. Mem., 1: 108–121

El-Akkad S, Abdallah AM (1971) Contribution to the geology of Gebel Ataqa area. Ann Geol Surv Egypt 1:21–42

El-Ayyat AM (2013) Sedimentology, sequential analysis and clay mineralogy of the lower Eocene sequence at Farafra Oasis area, Western Desert of Egypt. J Afr Earth Sci 78:28–50

Fairhead J, Guiraud R, Stone V (2003) Mesozoic plate tectonic controls on rift basin development on north central Africa: a major Cretaceous basin system. A.A.P.G. Annual Meeting 2003: Energy our monumental task, Salt Lake City, 12–14 April (Abstract), 4p

Farag IM, Ismail MM (1959) A contribution to the structure of the area east of Helwan. Egypt J Geol 3:71–86

Flügel E (1982) Microfacies analysis of limestones. Springer Berlin Heidelberg New York, 633p

Flügel E (2004) Microfacies of carbonate rocks: analysis, interpretation and application. Springer Berlin Heidelberg New York, 976p

Friedman GM, Sanders JE (2000) Comments about the relationships between new ideas an geologic terms in stratigraphy and sequence stratigraphy with suggested modifications. AAPG Bull 84(9):1274–1280

Garcia A (1994) Charophyta: their use in paleolimnology. J Paleolimnol 10:43–52

Gebelein CD, Steinen RP, Garrette P, Hoffman EJ, Plumer LN (1980) Subsurface dolomitization beneath the tidal flats of central west Andros Island. Bahamas. In: Zenger DH, Dunham JB, Ethington RH (eds) Concepts and models of dolomitization, Spec. Publ., Soc. Econ. Paleont. Miner., 28: 31–49

Geel T (2000) Recognition of stratigraphic sequences in carbonate platform and slope deposits: empirical models based on microfacies analysis of Paleogene deposits in southeastern Spain. Palaeogeogr Palaeoclimatol Palaeoecol 155:211–238

Grosjean AS, Pittet B (2013) Facies analysis and depositional environments of the Taulanne Limestone Formation in the South Alpine Foreland Basin (Oligocene, southeastern of France). Facies 59: 717–736

Guiraud R (1986) Correlations entre les principaux evenments geodynamiques enregistres du Trias a'nos jours sur les marges alpine et atlantique de la plaque africaine. Rev. Fac., Sc., Marrakech Sect. Sci., Terre. No. Spec. 2 PICG – UNESCO, 183: 313–338

Haggag W (2010) Structural setting an tectonic evolution of Gebel Shabrawet area and environs, north Eastern Desert, Egypt. Ph.D. Thesis, Fac. Sci., Geol. Dept., Benha Univ., 142p

Hallock P, Glenn E (1986) Larger foraminifera: a toll for paleoenvironmental analysis of Cenozoic carbonate depositional facies. Palaios 1:55–64

Handford CR, Loucks RG (1993) Carbonate depositional sequences and systems tracts-responses of carbonate platforms to relative sea-level changes. In: Loucks RG, Sarg JF (eds) Carbonate sequence stratigraphy. Recent events and applications. A.A.P.G., Mem., 57: 3–41

Haq BU, Hardenbol J, Vail PR (1988) Mesozoic and Cenozoic chronostratigraphy and cycles of sea-level changes. In: Wilgus CK, Hastings BS, Kendall CG, Posamentier HW, Ross CA, Van Wagoner JC (eds) Sea-level changes: an integrated approach. Society of Economic, Paleontologists and Mineralogists, special Publ., 42: 71–108

Hottinger L (1997) Shallow benthic foraminiferal assemblages as signals for depth of their deposition and limitations. Bull Soc Geol Fr 168: 491–505

Huerta P, Armenteros I (2005) Calcrete and palustrine assemblages on a distal alluvial-floodplain: a response to local subsidence (Miocene of the Duero Basin, Spain). Sediment Geol 177:235–270

Issawi B, Francis M, Youssef A, Osman R (2009) The Phanerozoic of Egypt: a geodynamic approach. Geol. Surv. Egypt, Spec. Publ., no. 81, 589p

Khalifa MA (1981) Geological and sedimentological studies of west Beni Mazar area, south El Fayium Province, Western Desert, Egypt. Ph.D. Thesis, Cairo University

Khalifa MA (1996) Depositional cycles in relation to sea level changes, case studies from Egypt and Saudi Arabia. Egypt J Geol 40(1):141–171

Kraus MJ (1999) Paleosols in clastic sedimentary rocks: their geologic applications. Earth Sci Rev 47:41–70

Kraus MJ, Aslan A (1993) Eocene hydromorphic paleosols: significance for interpreting ancient floodplain processes. J Sediment Res 63: 453–463

Krenkel E (1925–1934) Geologie der Erde. Geologie Afrikas, 3 volumes in 1925 (461p), 1928 (p. 463–1000), 1934 (p. 1003–1304). Berlin, Gebruder, Borntraeger

Marriott SB, Wright VP (1993) Paleosols as indicators of geomorphic stability in two Old Red Sandstone alluvial suites, South Wales. J Geol Soc Lond 150:1109–1120

Mohammad MH, Omran MA (1991) Stratigraphy and depositional history of the sedimentary sequence at Shabrawet area, southern Ismailia, Egypt. M.E.R.C., Ain Shams Univ., Earth Sci. Ser., 5: 16–30

Moustafa AR, Khalil MH (1989) North Sinai structures and tectonic evolution. M.E.R.C., Ain Shams Univ., Earth Sc. Ser., 3: 215–231

Osman R (2003) New findings in the Eocene stratigraphy of Gebel Ataqa–northern Galala, north Eastern Desert, Egypt. J Sediment Egypt 11:95–109

Pettijhon FJ, Potter PE, Siever R (1973) Sand and sandstone. Springer-Verlag New York, Heidelberg, 618p

Platt NH, Wright VP (1991) Lacustrine carbonates: facies models, facies distributions and hydrocarbon aspects. In: Anadón A, Cabrera Ll,

Kelts K (eds) Lacustrine facies analysis: International Association Sedimentologists Special Publication 13: 57–74

Platt NH, Wright VP (1992) Palustrine carbonates at the Florida Everglades: towards an exposure index for the freshwater environment. J Sediment Petrol 62:1058–1071

Sadek H (1926) The geology and geography of the district between Gebel Ataqa and El Galala El Bahariya. Egypt Geol. Surv. Dept., 120p

Said R (1960) Planktonic foraminifera from the Thebes Formation, Luxor, Egypt. Micropaleontology 6:277–286

Said R (1962) The geology of Egypt. New York, Amsterdam, 370p

Said R (1990) The geology of Egypt. Balkema, 734p

Said R, Issawi B (1964) Geology of northern plateau, Bahariya Oasis. Egypt Geol. Surv., paper 28, 41p

Said R, Martin L (1964) Cairo area, geological excursion notes. Six Annual Field Conf., Petrol. Explor. Soc. Libya, Elsevier, 107–121

Sallam E, Issawi B, Osman R (2015) Stratigraphy, facies and depositional environments of the Paleogene sediments in Cairo-Suez district, Egypt. Arab J Geosci 8:1939–1964

Sarg JF (1988) Carbonate sequence stratigraphy. In: Wilgus CK, Hastings BS, Kendall CG, Posamentier HW, Ross CA, Van Wagoner JC (eds) Sea-level changes: an integrated approach. Society of Economic, Paleontologists and Mineralogists, special Publ., 42: 155–181

Schlager W (2005) Carbonate sedimentology and sequence stratigraphy. Soc Sediment Geol Concepts Sedimentol Paleontol 8:200

Selim SS, El Araby AA, Darwish M, Abu Khadrah AM (2012) Anatomy and development of tectonically-induced Middle Eocene clastic wedge on the southern Tethys Shelf, north Eastern Desert, Egypt. GeoConvension 2012: Vision, 1–6

Shamah K, Helal S (1993a) Benthic foraminifera from Gebel El-Goza El-Hamra and its neighbourhood, Suez-Canal zone, Egypt. Ann Geol Surv Egypt 19:245–260

Shamah K, Helal S (1993b) Stratigraphy of the Eocene sediments at Shabrawet area, Suez Canal environs, Egypt. Egypt J Geol 37(2): 275–298

Sim LL, Chambers JM, Davis JA (2006) Ecological regime shifts in salinised wetland systems. I. Salinity thresholds for the loss of submerged macrophytes. Hydrobiology 573:89–107

Soulié-Märsche I (2008) Charophytes, indicator for low salinity phases in North African sebkhet. J Afr Earth Sci 51:69–76

Stefan H, Scheibner C, Kuss J, Marzouk AM, Rasser MW (2011) Tectonically driven carbonate ramp evolution at the southern Tethyan shelf: the Lower Eocene succession of the Galala Mountains, Egypt. Facies 57:51–72

Sztrakos K (2000) Les Foraminifères de l'Eocène du basin de l'Adour (Aquitaine, France): biostratigraphie et taxonomie. Re. Micopaléont., Paris, 42/1-2, p. 71–172

Sztrakos K (2001) La Stratigraphie du Paléogène européen. Deux examples: les basins paléogènes de la Hongrie et de l'Aquitaine. Mém. H.D.R., Univ. Paris, 43p

Tucker ME, Wright VP (1990) Carbonate sedimentology. Blackwell Science, Oxford, 482p

Vail PR, Mitchum RM, Todd RG, Widmier JM, Thomposon III S, Sangree JB, Bubb JN, Hatfield WG (1977) Seismic stratigraphy and global changes in sea level. In: Payton CE (ed) Seismic stratigraphy—application to hydrocarbon exploration. AAPG Memoir 26: 49–212

Van Wagoner JC, Posamentier HW, Mitchum RM, Vail PR, Sarg JF, Loutit TS, Hardenbol J (1988) An overview of the fundamentals of sequence stratigraphy and key definitions. In: Sea-level changes. An integrated approach, SEPM, special publ., 42: 39–45

Wanas HA (2008) Cenomanian rocks in the Sinai Peninsula, northeast Egypt: facies analysis and sequence stratigraphy. J Afr Earth Sci 52: 125–138

Wanas HA, Abu El-Hassan MM (2006) Paleosols of the Upper Cretaceous–Lower Tertiary Maghra El-Bahari in the northeastern portion of the Eastern Desert, Egypt: their recognition and geological significance. Sediment Geol 183:243–259

Wanas HA, Soliman HE (2014) Calcretes and palustrine carbonates in the Oligo-Miocene clastic–carbonate unit of the Farafra Oasis, Western Desert, Egypt: their origin and paleoenvironmental significance. J Afr Earth Sci 95:145–154

Wilson JL (1975) Carbonate facies in geologic history. Springer, New York, 471p

Ziegler PA (1990) Geological atlas of Western and Central Europe, 2edth edn. Shell Int. Petrol. Mij. B.V. and Geol. Soc, London, 239p

Ziegler PA, Cloethingh S, Guiraud R, Stampfli GM (2001) Peritethyan platforms constraints on dynamics of rifting and basin inversion. In: Zeigler PA, et al. (eds) Peri-tethyan Mem. 6: Peri-tethyan rift/wrench basins and passive margins. Mém. du Muséum National d'Hist. Nat. de Paris, 186: 9–49